OPEN-FILE REPORT 04-1

Evaluation of Bottom-Hole Temperatures in the Canon City Embayment, Hugoton Embayment, North Park, Paradox, Piceance, Raton, and Sand Wash Basins of Colorado

By Jeanette Dixon

COLORADO
DEPARTMENT OF NATURAL RESOURCES

Bill Owens, Governor,
State of Colorado

Russell George, Executive Director,
Department of Natural Resources

COLORADO DIVISION OF MINERALS & GEOLOGY
RECLAMATION•MINING SAFETY•SCIENCE

Ronald W. Cattany, Director,
Division of Minerals and Geology

COLORADO GEOLOGICAL SURVEY

Vince Matthews, State Geologist

Colorado Geological Survey
Division of Minerals and Geology
Department of Natural Resources
Denver, Colorado/2004

FOREWORD

The purpose of the Colorado Geological Survey Open File Report 04-1 is to create a bottom-hole temperature (BHT) database and analyze the data for reliability and geologic trends. The Canon City, Hugoton, North Park, Raton, Paradox, Piceance, and Sand Wash Basins were studied in order to complete a state-wide study of BHTs. This study is a companion study to Open File Report 02-15, *Evaluation of Bottom-Hole Temperatures in the Denver and San Juan Basins of Colorado*. The bottom-hole temperatures were entered into a Colorado Oil and Gas Conservation Commission database, graphed in Excel™ and mapped in Petra™ and ArcView™. The objective of this publication is to provide a bottom-hole temperature database and analysis to resource developers and interested citizens.

Funding for this project came from the Colorado Department of Natural Resources Severance Tax Operational Fund. Severance taxes are derived from the production of gas, oil, coal, and minerals.

James A. Cappa
Chief, Mineral and Mineral Fuels Section

Vince Matthews
State Geologist

Ronald W. Cattany
Director, Division of Minerals and Geology

ACKNOWLEDGEMENTS

I wish to thank a number of people who helped with the study: Jim Cappa, Cheryl Brchan, Chris Martin, and Vanessa Graves for their technical guidance and assistance. I thank the Colorado Oil and Gas Conservation Commission for providing the well database and microfilm from which the data was recorded.

CONTENTS

FIGURES

APPENDIX A

Well Data Files

- Canon City Embayment
- Hugoton Embayment
- North Park Basin
- Paradox Basin
- Piceance Basin
- Raton Basin
- Sand Wash Basin

INTRODUCTION

The maximum recorded temperature or bottom-hole temperature (BHT) is usually recorded when logging an oil or gas well. It is used in wellbore management, oil and gas prospecting, and reservoir analysis for calculating reserves. Edwardson, and others (1962), Middleton (1982), Fertl and Wichmann (1977), and Fertl (1978, 1985) have described various influences on the measured BHT and how to calculate a true temperature, compensating for those influences. Bottom-hole temperatures were studied by Dixon (2002) to see if the raw, unadjusted temperatures could be of value. In both the Denver Basin and the San Juan Basin of Colorado, data indicated an increase in temperature possibly related to deep basement structures.

The purposes of this study are to complete a statewide bottom-hole temperature database (in conjunction with Colorado Geological Survey OFR 02-15, *Evaluation of bottom-hole temperatures in the Denver and San Juan Basins of Colorado*) and to determine if any geologic trends noticeably influence BHTs in the Canon City, Hugoton, North Park, Paradox, Piceance, Raton, and Sand Wash basins. Detailed analyses are beyond the scope of this project.

A total of 5,039 BHTs were recorded for the seven basins included in this study. These BHTs, in combination with the 10,908 BHTs acquired in the Denver and San Juan basins study, make a database of 15,946 bottom-hole temperatures for the nine oil and gas basins of Colorado (Fig. 1). This is a statewide BHT sampling rate of over one-fourth of the oil and gas wells in the Colorado Oil and Gas Conservation Commission (COGCC) database.

DATA ACQUISITION AND ANALYSIS

The well database from the COGCC was downloaded from the Internet and loaded into Excel™ spreadsheets by county. In each county, well log headers from microfilm were used to obtain maximum temperatures and hours-since circulation data. In order to be consistent, maximum temperatures were recorded from induction logs since they were the logs most widely available. Corrections for driller total depth, logger total depth, and reference elevations were made if necessary. In some areas, BHTs were not consistently recorded or were recorded as " less than 100°F." The county spreadsheets were then divided into basins. In some cases, data points fell outside the basin outlines or did not have all necessary data and were not included in the basin studies, but are included in the BHT database (Appendix A). Great effort was made to accurately collect the data. However, the data itself may contain operator and mechanical errors and caution should be used when analyzing the data.

Plots of elevation at total depth-versus-maximum temperature were made in Excel™ for each basin. Additional graphs were made in some basins to analyze particular trends. No mathematical corrections or calculations were made on the data. In a previous study by Dixon (2002), normalization of bottom-hole data appeared to introduce as many errors as it might correct, at least on a basin-wide study. In most basins, there is an insufficient distribution of data on any single formation to make a meaningful contour map. However, in the Sand Wash and Piceance basins, there is a fair distribution of data. In those basins, BHTs were loaded into Petra™ and contoured. The BHT contours by formation at total depth were then compared to basement structures as mapped by Hemborg (1996) (Fig. 2) to see if the BHTs might be influenced by deep structures. Stratigraphic columns used were after Ambrose (1998).

CANON CITY EMBAYMENT

The Canon City Embayment is a Laramide, synclinal graben located southwest of the Denver Basin. It is bounded on the north by the Front Range Uplift, on the south by the Apishapa Uplift, and on the southwest by the Wet Mountains Uplift (Fig. 3). The basin is deepest on the west side, reaching Precambrian basement rocks at an elevation just below sea level.

Bottom-hole temperatures were recorded from stratigraphic formations ranging from the Precambrian to the Pierre Shale (Fig. 4). They were then plotted by elevation at total depth-versus-maximum temperature (Fig. 5). Basin-wide recording of temperatures was generally poor. The data were somewhat scattered, but there were too few points to draw any conclusions. No further analysis was made in the basin.

HUGOTON EMBAYMENT

The Hugoton Embayment of Colorado lies in the southeast part of the state. It is bounded on the north by the Las Animas Arch and on the west by the Apishapa Uplift. The configuration of the southeastern part of Colorado was shaped mostly by Laramide uplifting (Fig. 6). The deepest part of the Hugoton Embayment in Colorado is about 3,200 feet below sea level.

Temperatures were recorded from Precambrian to Pennsylvanian strata (Fig. 7), but the majority were from the Mississippian and Pennsylvanian rocks. Graphs were made comparing elevation at total depth versus maximum temperature for all wells, by operator, and by formation (Fig. 8, 9, and 10). The overall temperature gradient is a little less than 1°F per 1000 feet. BHTs tended to cluster when comparing temperatures by formation. When comparing temperatures by operator, some linear trends might cause concern for the method by which temperatures were recorded.

NORTH PARK BASIN

North Park Basin is the northern-most basin of the north-south-trending Laramide structural basins located in north-central Colorado. The basin is bounded on the east by the Front Range Uplift and on the west by the Park Range. Tertiary intrusive and volcanic rocks separate North Park and Middle Park basins. The deepest part of the basin is on the east side at about 5,000 feet below sea level (Fig. 11).

The majority of the temperatures in this basin came from the Upper Jurassic and Lower Cretaceous formations (Fig. 12). The over-all temperature gradient is a little over 1°F per 1000 feet (Fig. 13). A graph with temperatures plotted by formation shows that there is little difference in temperature gradients between the four main formations (Fig. 14).

PARADOX BASIN

The Paradox Basin is situated in southwest Colorado and in southeast Utah with a small portion located in northeast Arizona. The basin is bounded on the northeast by the Uncompahgre Uplift. The San Juan volcanic field is to the east of the basin. The deepest part of the Colorado part of the basin is in the northeast, paralleling the Uncompahgre Uplift. The basement rocks are greater than 15,000 feet below sea level (Fig. 15).

BHTs recorded in this basin came mainly from the Mississippian and Pennsylvanian formations (Fig. 16). The plot of elevation at total depth-versus-maximum temperature for all BHTs in the Paradox Basin shows a greater scatter in temperatures than in some other basins. The over-all temperature gradient is about 0.9°F per 1000 feet (Fig. 17). A plot of BHTs by formation indicates that most of the scatter in the data is in the Paradox Formation (Fig. 18).

PICEANCE BASIN

The Piceance Basin of Colorado is a northwest-southeast trending basin situated on the western side of Colorado. It is bounded on the northeast by the Axial Uplift, on the east by the White River Uplift, and on the southwest by the Uncompahgre Uplift. It is separated from the Uinta Basin of Utah by the Douglas Creek Arch. The deepest part of the basin is on the east side near the White River Uplift. The top of the basement rocks there is about 15,000 feet below sea level (Fig. 19).

Significant oil and gas deposits are found throughout the section from the Pennsylvanian to the Tertiary (Fig. 20). The temperature gradient determined from a plot of all wells is about 1.3°F per 1000 feet (Fig. 21). A plot of BHTs by operator shows normal scatter in temperatures and does not show linear trends as seen in the Hugoton Embayment data (Fig. 22).

There are sufficient numbers and distribution of data to contour some BHTs by formation at total depth in the Piceance Basin. The Mancos Shale bottom-hole temperatures were contoured. A comparison of BHT contours with basement structure contours show a good correlation between BHTs and depth to basement (Fig. 23). Additionally, those contours were compared to vitrinite isoreflectance trends on the Mancos Shale (Fig. 24). All three contour trends reflect the relationship between the overall thickness of the sediments and the depth to basement with the temperatures and maturity of the formations. This indicates, as in previous studies, that raw, unadjusted bottom-hole temperatures can reflect true formation temperatures and can be used, in some cases, for exploration and evaluation of formations.

BHTs of the Mesaverde and Weber formations were contoured (Fig. 25 and Fig. 26). These contours also show a relationship between the temperatures and depth to basement. Other formations did not have a good enough distribution of data to make meaningful contour maps.

RATON BASIN

The Raton Basin is located in south-central Colorado and north-central New Mexico. In Colorado, the basin is bounded on the west by thrust faulting associated with the Sangre de Cristo Uplift, the Wet Mountains on the north, and the Apishapa Arch on the northeast side, and the Las Animas Uplift on the east side. The deepest part of the basin in Colorado is in the southern part. Hemborg (1996) maps the basement rocks there below 2000 feet below sea level (Fig. 27).

Formations at total depth range in age from Pennsylvanian to Late Cretaceous (Fig. 28). A plot of BHTs from all wells show a fair scatter in temperatures (Fig. 29). The temperature gradient for all wells is about 1.2°F per 1000 feet. When comparing BHTs by operator, some of the data scatter may be caused by recording methods, for example: some of the greatest data scatter is recorded by just one company. Also, linear trends in BHTs are seen by two operators giving rise to question recording methods (Fig. 30). Finally, temperatures were plotted comparing the CO_2 wells of Sheep Mountain field to all other wells (Fig. 31). Although the CO_2 temperatures were somewhat scattered, the wells terminate in different formations and at different depths. The CO_2 wells of Sheep Mountain field were compared to the CO_2 wells of McElmo field in the Paradox Basin, and to one well in North Park Basin (Fig. 32). The McElmo temperatures were more concentrated in depth and appear more clustered than those of Sheep Mountain. However, the temperatures in both fields scatter around 150°F despite the some 4000 feet difference in depth.

SAND WASH BASIN

The Sand Wash Basin lies in northwest Colorado and southwest Wyoming. In Colorado, the basin is bounded by the Park Uplift to the west and by the White River Uplift to the south. The Uinta Uplift and the Axial Arch bounds the basin to the southwest (Fig. 33). The deepest part of the basin in Colorado is to the northwest at a depth greater than 15,000 feet below sea level.

Bottom-hole temperatures were recorded from Precambrian to upper Cretaceous rocks (Fig. 34) and plotted by elevation at total depth-versus-maximum temperature (Fig. 35). The overall temperature gradient is about 1.2°F per 1000 feet. BHTs were plotted by operator, using the two operators that had the most data recorded (Fig. 36). The scatter appeared normal and without linear trends seen in some of the other basin data sets.

A contour map of BHTs from the Mesaverde Group was compared to contours of basement structure (Fig. 37). The temperatures tend to be hotter in the deeper part of the basin, but there was not a good distribution of data to make a strong conclusion. No other formation was contoured because there was not a sufficiency or distribution of data to make a meaningful map.

CONCLUSIONS

Bottom-hole temperatures are useful data. It is important that they are always recorded accurately. Unfortunately, in some oil and gas basins of Colorado, those temperatures were not recorded and the data was lost. As seen in this study and the previous study of Colorado BHTs (Dixon, 2002), it is not always required that the temperatures be mathematically manipulated to be useful.

In the Hugoton and Raton Basins, plots of BHTs showed some linear trends by operator giving rise to the question of the method by which these data were recorded. Temperature gradients from all of the basins in this study range from 0.9°F to 1.3°F per 1000 feet. Contour maps in the Piceance and Sand Wash basins show good correlation between BHTs and depth to basement. In the Piceance Basin, BHT contours of the Mancos Shale, basement structure contours, and vitrinite isoreflectance contours on top of the Mancos Shale also show good correlation. In the Raton and Paradox basins, BHTs from CO_2 wells were scattered around 150°F even though the total depths varied by over 4000 feet.

CITED REFERENCES

Ambrose, C. M. T., 1998, Penetration charts of selected Colorado oil and gas fields: Colorado Geological Survey Resource Series 34.

Dixon, Jeanette, 2002, Evaluation of bottom-hole temperatures in the Denver and San Juan Basins of Colorado: Colorado Geological Survey Open-File Report 02-15.

Donatch, A. J. and Carter, L. M., editors, 2003, Petroleum systems and geologic assessment of oil and gas in the Unita-Piceance Province, Utah and Colorado: USGS Digital Data Series DDS-69-B, version 1.0.

Edwardson, M. J., Girner, H. M., Parkison, H. R., Williams, C. D., and Mathews, C. S., 1962, Calculation of formation temperature disturbances caused by mud circulation: Journal of Petroleum Technology, vol. 14, No. 4, April, 1962.

Fertl, W. H. and Wichmann, P. A., 1977, How to determine static BHT from well log data: World Oil, January 1977, p. 105-106.

Fertl, W. H., 1978, How subsurface temperature affects formation evaluation: Oil and Gas Journal, July 24, 1978, p. 54-62.

Fertl, W. H., 1985, Logs help approximate reservoir temperature: Oil and Gas Journal, April, 1985, p. 89-91.

Hemborg, H. T., 1996, Basement structure map of Colorado with major oil and gas fields: Colorado Geological Survey Map Series 30.

Middleton, M. F., 1982, Bottom-hole temperature stabilization with continued circulation of drilling mud: Geophysics, v. 47, n. 12, p. 1716-1723.

Wray, L. L., Apeland, A. D., Hemborg, H. T., and Brchan, C. A., 2002: Oil and gas fields map of Colorado: Colorado Geological Survey Map Series 33.

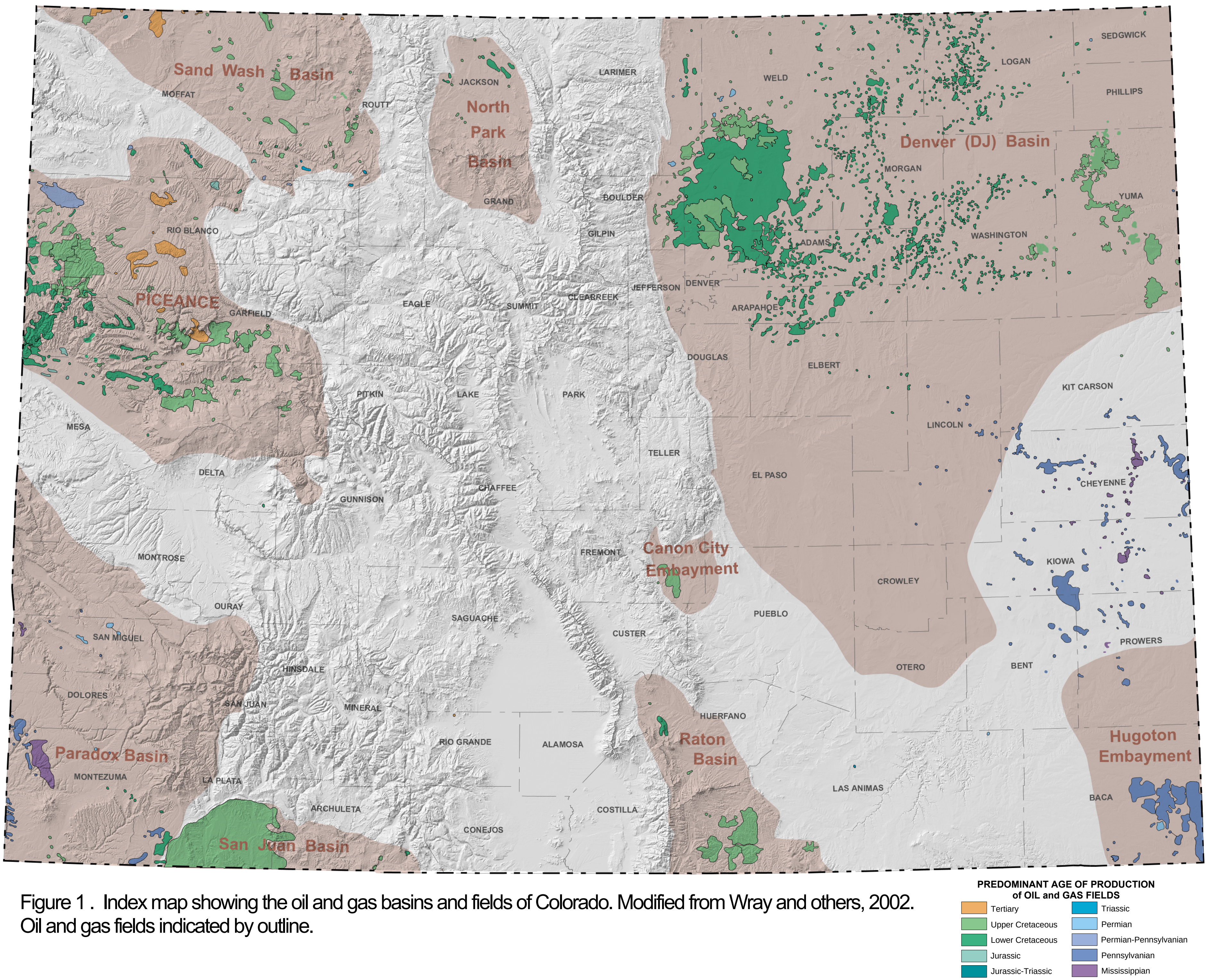

Figure 1 . Index map showing the oil and gas basins and fields of Colorado. Modified from Wray and others, 2002. Oil and gas fields indicated by outline.

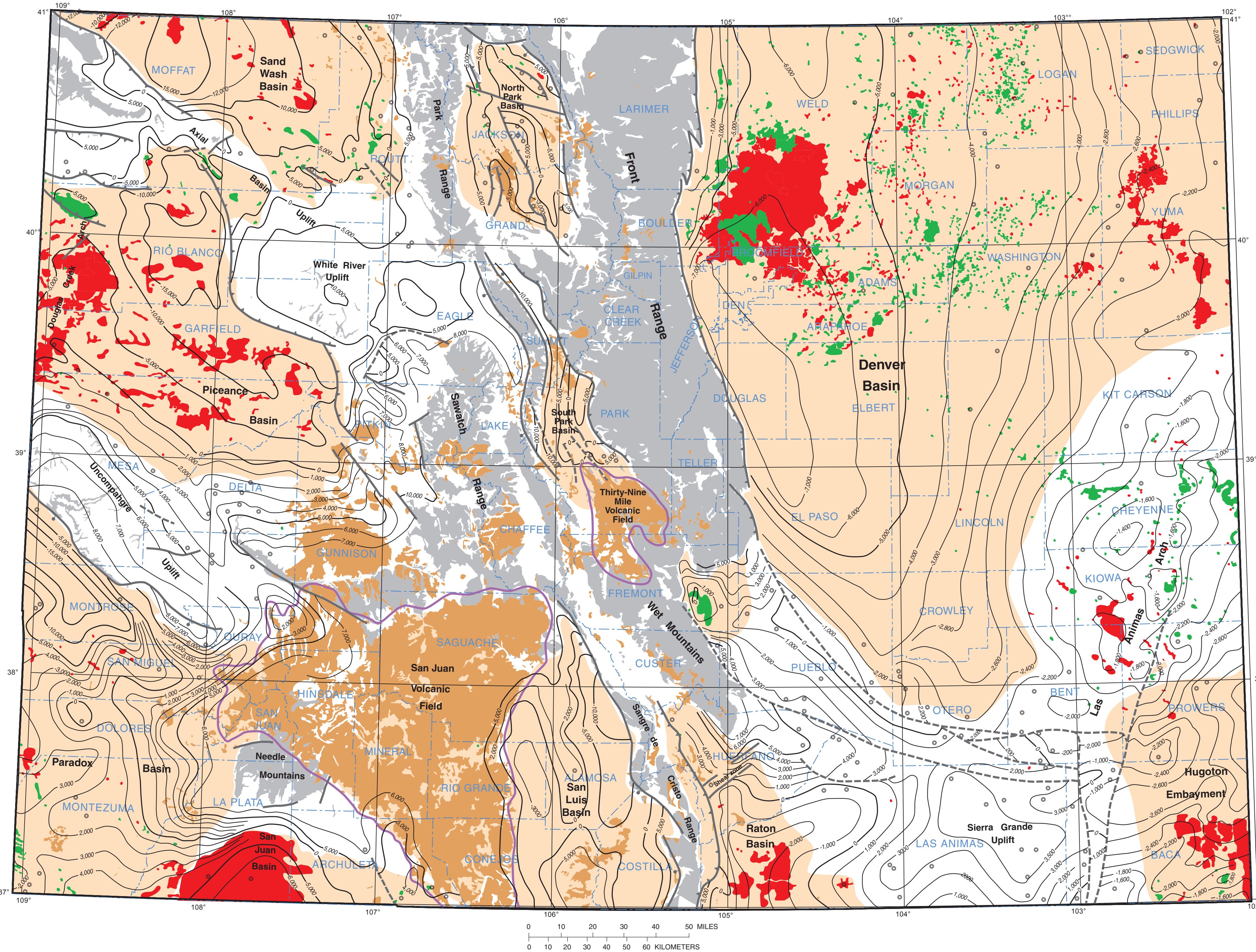

Figure 2. Basement structure map of Colorado with major oil (green) and gas (red) fields; Upper Cretaceous to Tertiary volcanic and intrusive rock outcrops (rust); faults; wells drilled to Precambrian basement rocks; undifferentiated Precambrian rock outcrop (gray); and structure contours on top of Precambrian basement rock in feet above or below sea level. Hemborg, 1996.

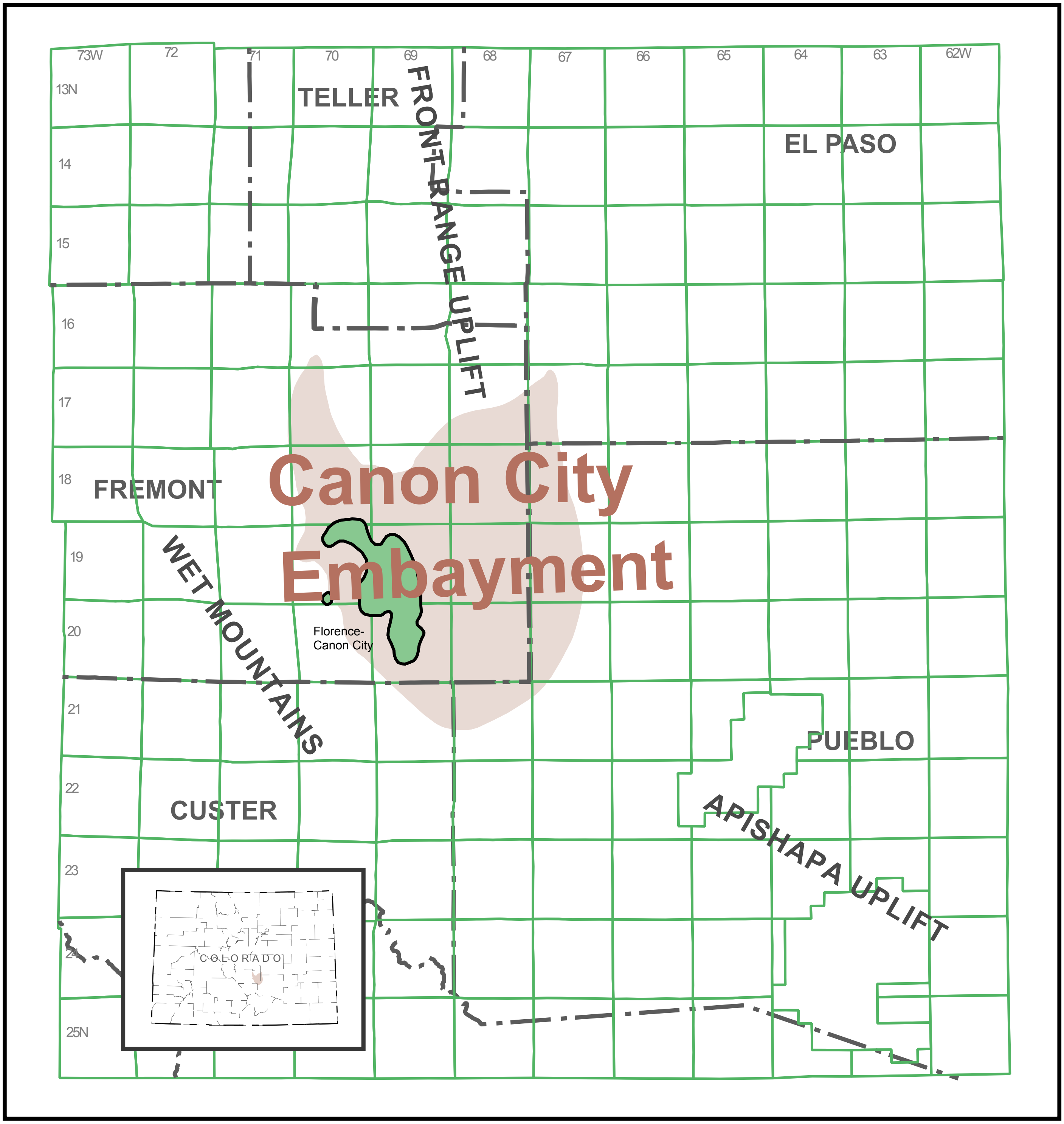

Figure 3. Map of the Canon City Embayment. After Wray and others, 2002. Oil and gas fields indicated by outline.

PREDOMINANT AGE OF PRODUCTION of OIL and GAS FIELDS

- Tertiary
- Upper Cretaceous
- Lower Cretaceous
- Jurassic
- Jurassic-Triassic
- Triassic
- Permian
- Permian-Pennsylvanian
- Pennsylvanian
- Mississippian

CANON CITY EMBAYMENT

AGE	STRATIGRAPHIC UNIT
PALEOCENE	Poison Canyon
	Raton Formation
UPPER CRETACEOUS	Vermejo Formation
	Trinidad Sandstone
	Pierre Shale
	Niobrara Formation
	Smoky Hill (Apishapa) Mbr
	Fort Hays (Timpas) Ls Mbr
	Carlile Shale
	Codell Sandstone Mbr
	Greenhorn Limestone
	Graneros Shale
LOWER CRETACEOUS	Dakota Sandstone
	Purgatorie Formation
UPPER JURASSIC	Morrison Formation
	Ralston Creek Formation
UPPER PERMIAN	Lykins Formation
	Lyons Formation
LOWER PERMIAN / PENNSYLVANIAN	Fountain Formation
PENNSYLVANIAN	Glen Eyrie Member
MISSISSIPPIAN	Beulah Limestone
	Hardscrabble Limestone
	Williams Canyon Limestone
ORDOVICIAN	Fremont Dolomite
	Harding Sandstone
	Manitou Limestone
PRECAMBRIAN	Precambrian rocks

Figure 4. Stratigraphic section of the Canon City Embayment. After Ambrose, 1998.

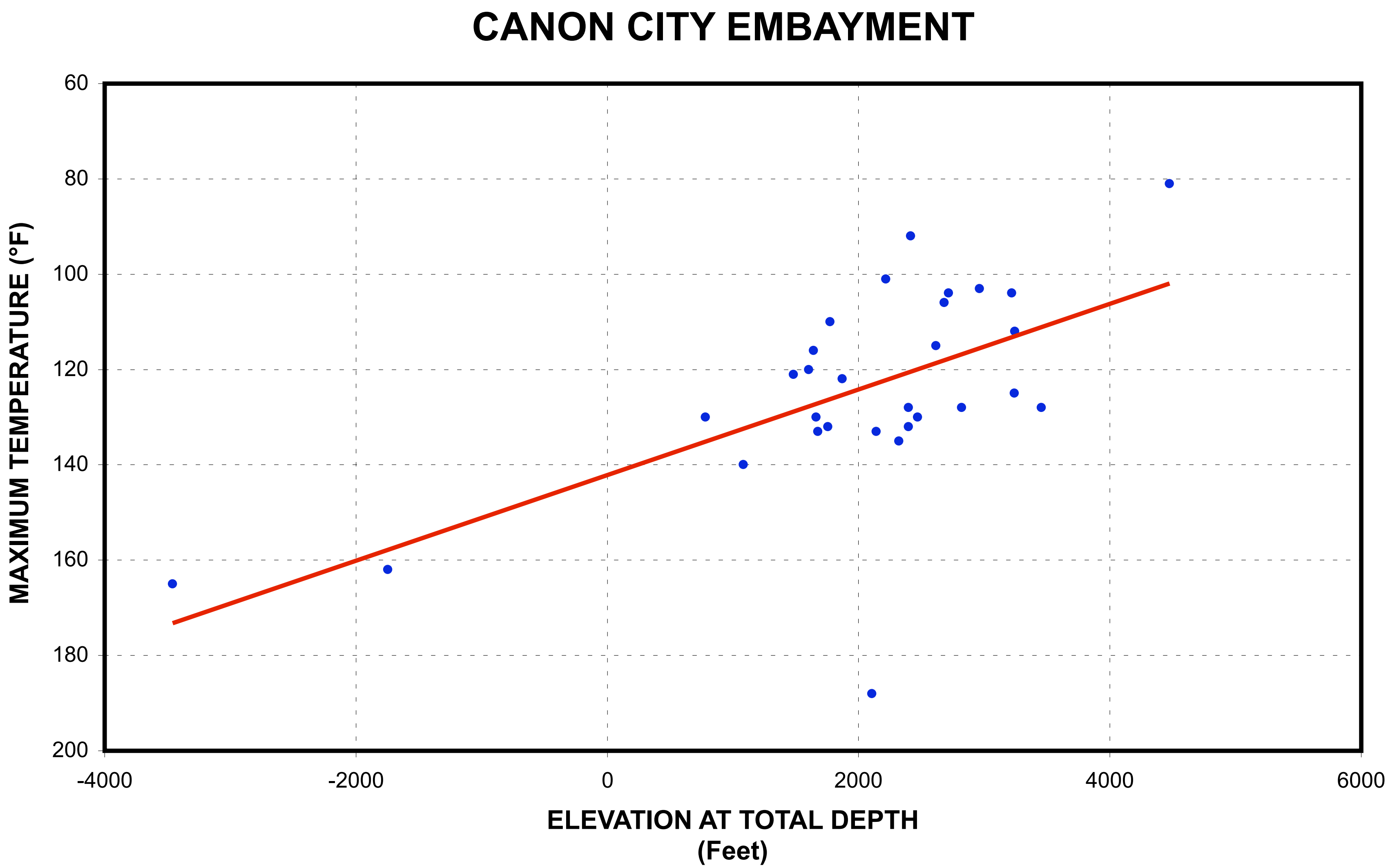

Figure 5. Plot of elevation at total depth-versus-maximum temperature, all wells.

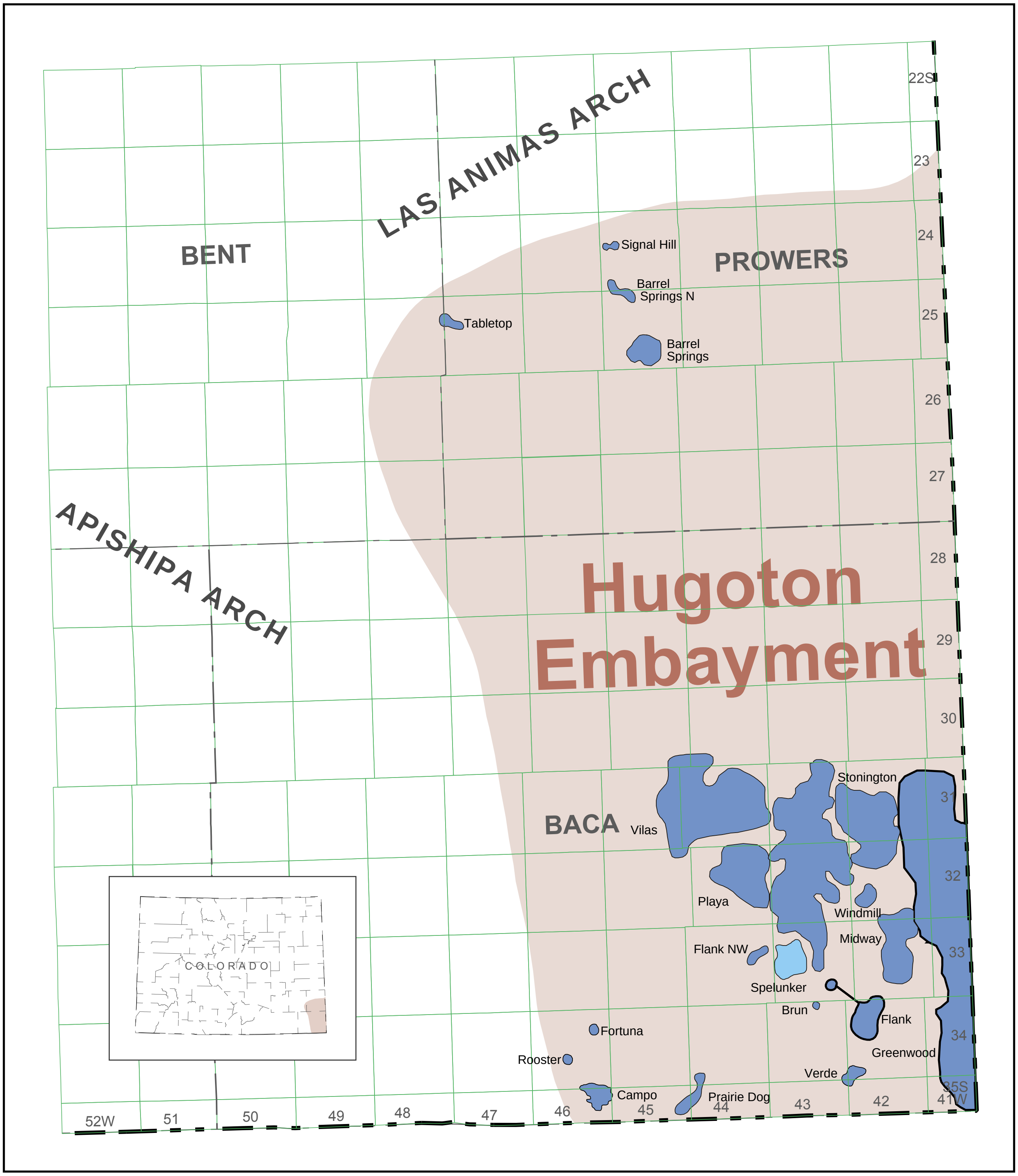

Figure 6. Map of the Hugoton Embayment. After Wray and others, 2002. Oil and gas fields indicated by outline.

PREDOMINANT AGE OF PRODUCTION of OIL and GAS FIELDS

Tertiary	Triassic
Upper Cretaceous	Permian
Lower Cretaceous	Permian-Pennsylvanian
Jurassic	Pennsylvanian
Jurassic-Triassic	Mississippian

HUGOTON EMBAYMENT

AGE		STRATIGRAPHIC UNIT
QUATERNARY		Eolian deposits
PLIOCENE		Ogalla Group
MIOCENE		
LOWER CRETACEOUS		Dakota Group
JURASSIC		Morrison Formation
TRIASSIC		Dockum Group
UPPER PERMIAN		Taloga Formation
		Day Creek Dolomite
		Whitehorse Group
		Blaine Gypsum Mbr (Lykins)
		Nippewalla Group
		Cedar Hills Sandstone (Lyons)
LOWER PERMIAN		Stone Corral Sandstone
		Sumner Group
		Red Cave Formation
	Wolfcampian	Chase Group
		Council Grove Grroup
		Neva Limestone
PENNSYLVANIAN	Virgilian	Admire Group
		Wabaunsee Formation
		Shawnee Group
		Topeka Member
		Heebner Member
		Douglas Group
	Missourian	Lansing Group
		Kansas City Group
		Pleasanton Group
	Des Moinesian	Marmation Group
		Cheerokee Group
		Atoka Group
		Morrow Group
UPPER MISSISSIPPIAN		Chester Group
		St. Genevieve Limestone
		St. Louis Limestone
		Spergen Limestone
		Warsaw Limestone
LOWER MISSISSIPPIAN		Osage Limestone
		Kinderhook Limestone
		Misener Sandstone
MIDDLE ORDOVICIAN		Viola Limestone
		Simpson Group
LOWER ORDOVICIAN		Arbuckle Group
UPPER CAMBRIAN		Reagan Sandstone
PRECAMBRIAN		Precambrian rocks

Figure 7. Stratigraphic section of the Hugoton Embayment. After Ambrose, 1998.

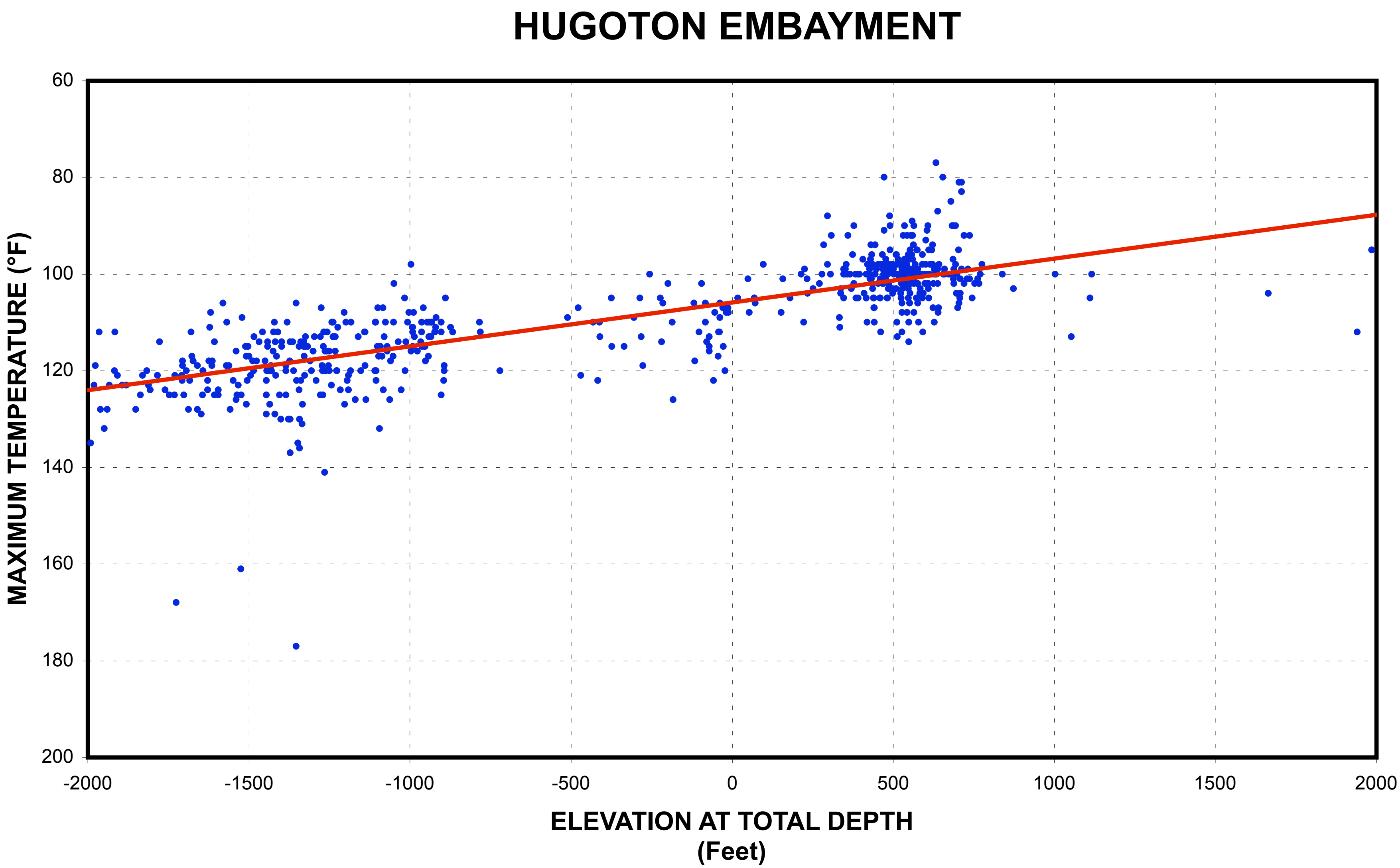

Figure 8. Plot of elevation at total depth-versus-maximum temperature, all wells.

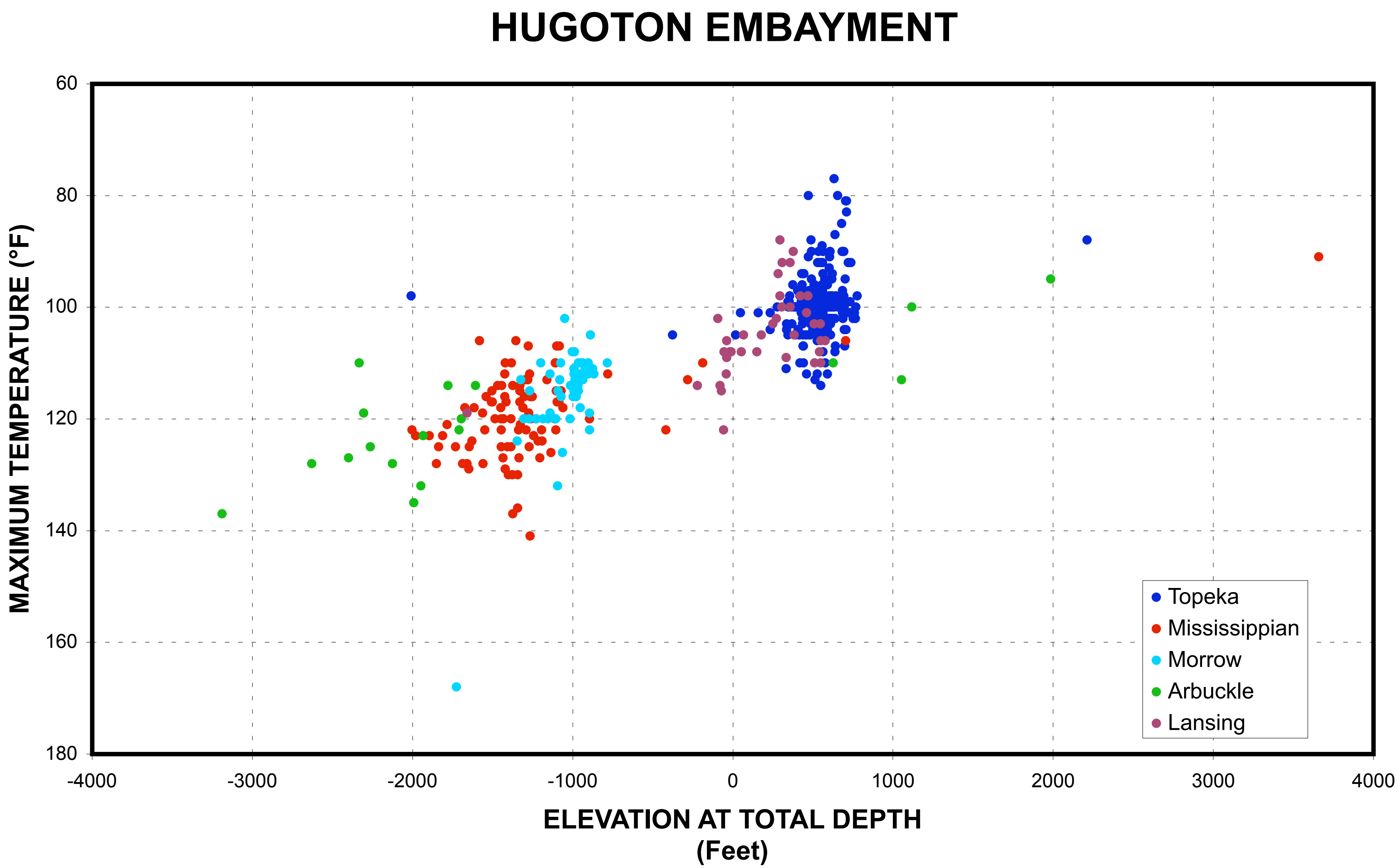

Figure 9. Plot of elevation at total depth-versus-maximum temperature, by formation.

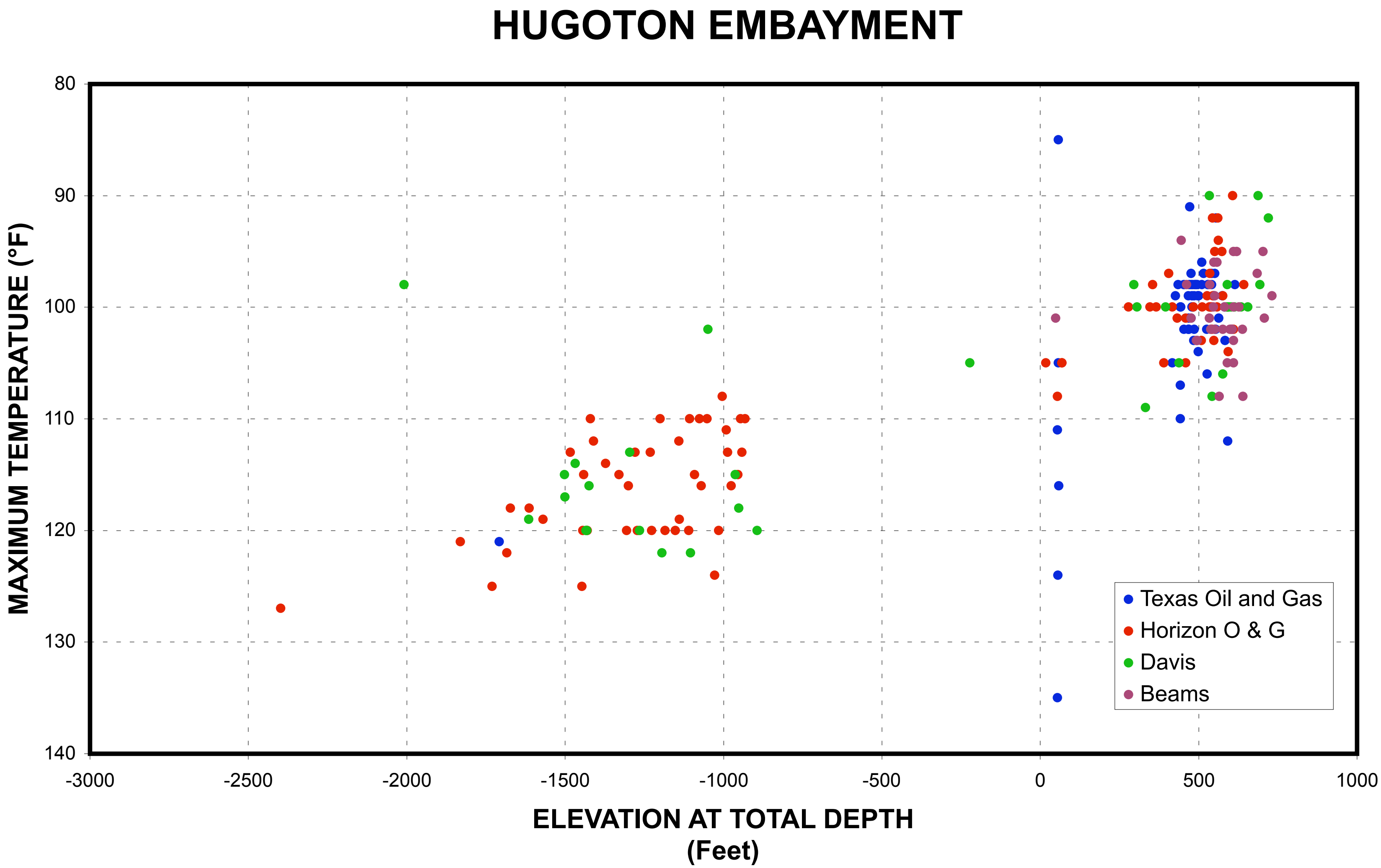

Figure 10. Plot of elevation at total depth-versus-maximum temperature, by operator.

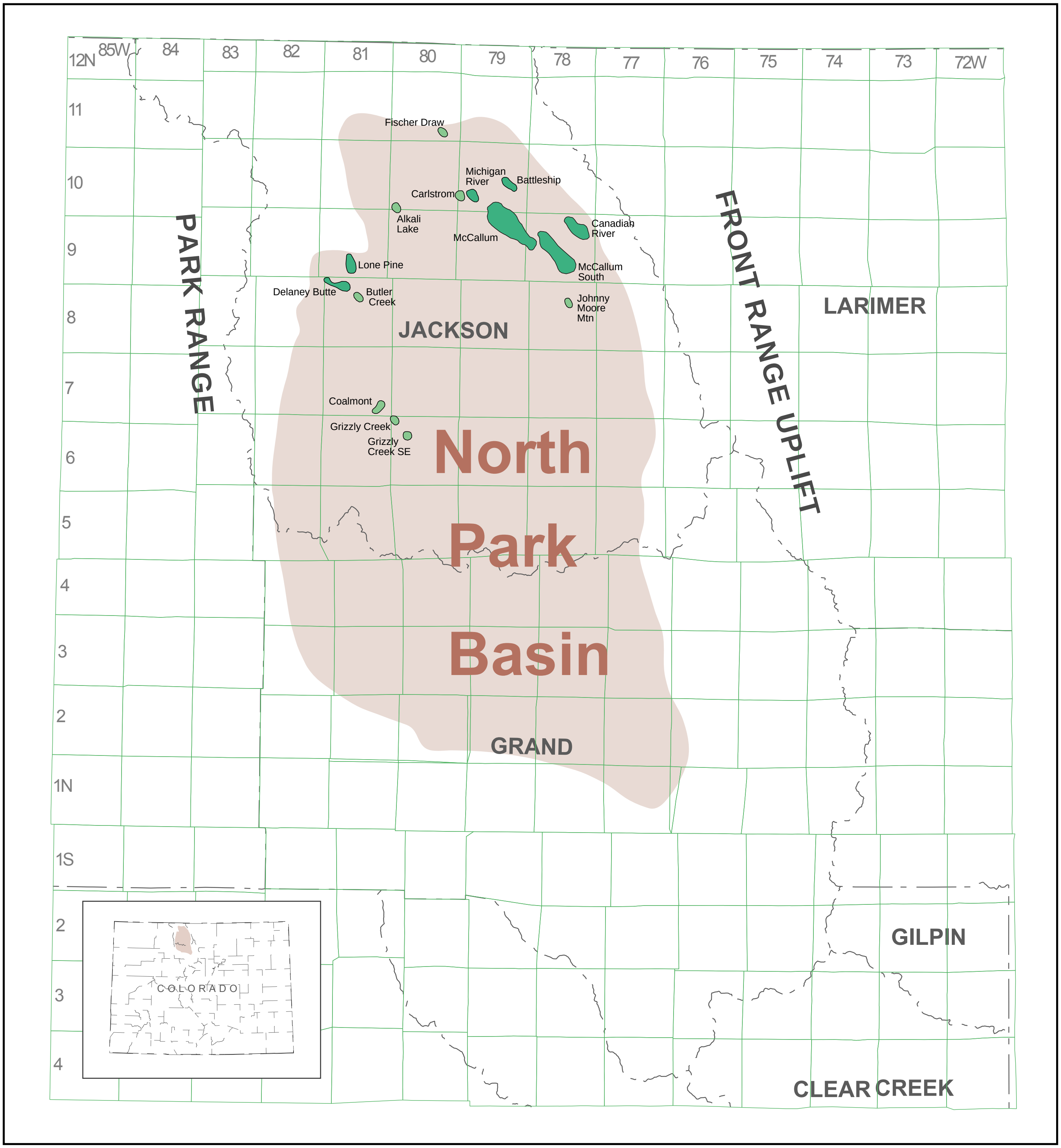

Figure 11. Map of the North Park Basin. After Wray and others, 2002. Oil and gas fields indicated by outline.

PREDOMINANT AGE OF PRODUCTION of OIL and GAS FIELDS

- Tertiary
- Upper Cretaceous
- Lower Cretaceous
- Jurassic
- Jurassic-Triassic
- Triassic
- Permian
- Permian-Pennsylvanian
- Pennsylvanian
- Mississippian

NORTH PARK BASIN

AGE	STRATIGRAPHIC UNIT
EOCENE	Coalmont Formation
PALEOCENE	
UPPER CRETACEOUS	Pierre Shale
	Niobrara Formation
	Carlile shale
	Frontier Formation
	Graneros Shale
	Mowry Shale
	Muddy Sandstone
LOWER CRETACEOUS	Dakota Group
	Dakota Sandstone
	Fuson Sand
	Lakota Sandstone
UPPER JURASSIC	Morrison Formation
	Sundance (Entrada) Formation
TRASSIC	Jelm Formation
	Chugwater Formation
PRECAMBRIAN	Precambrian rocks

Figure 12. Stratigraphic section of the North Park Basin. After Ambrose, 1998.

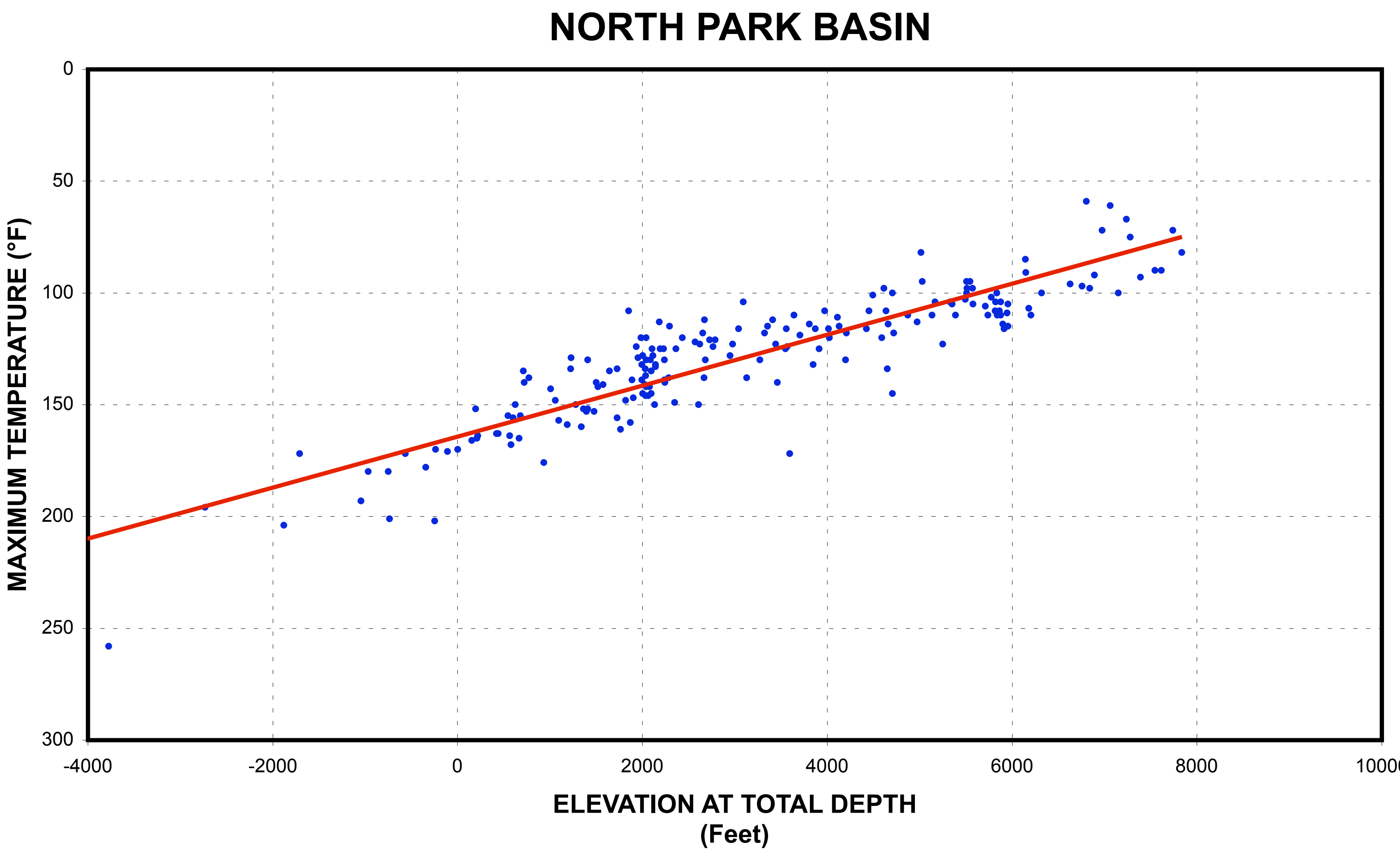

Figure 13. Plot of elevation at total depth-versus-maximum temperature, all wells.

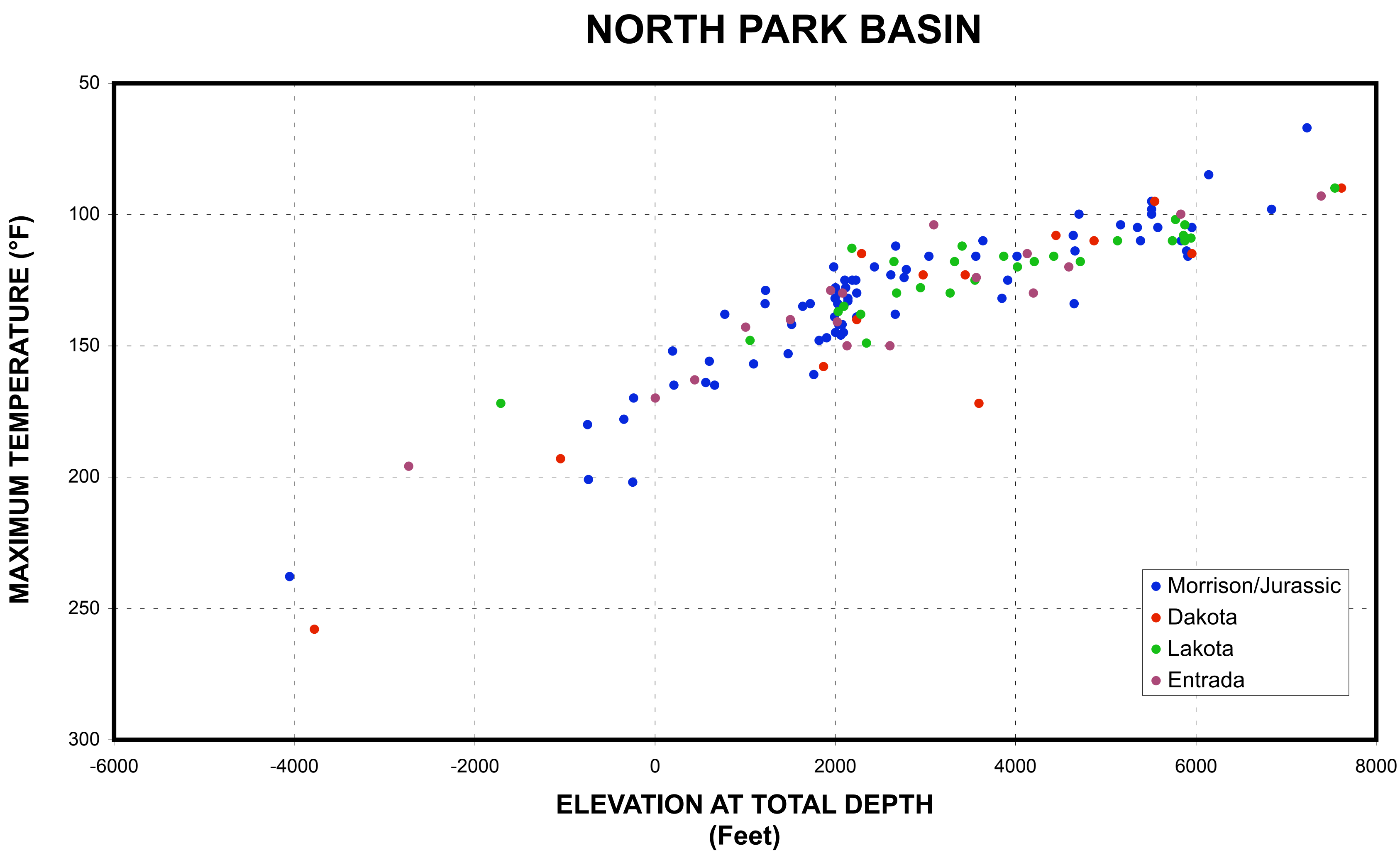

Figure 14. Plot of elevation at total depth-versus-maximum temperature by individual formation.

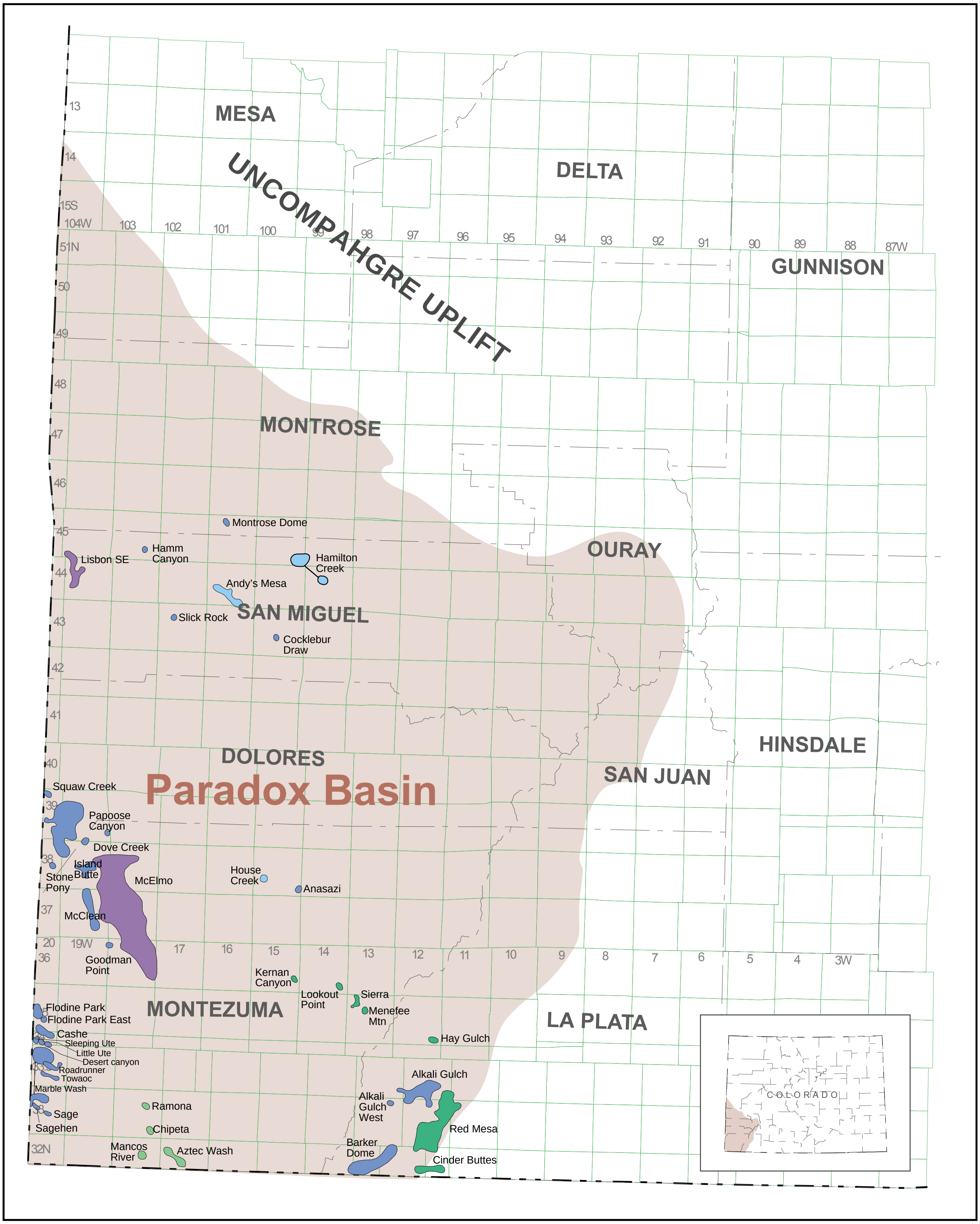

Figure 15. Map of the Paradox Basin. After Wray and others, 2002. Oil and gas fields indicated by outline.

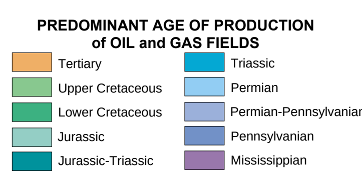

PARADOX BASIN

AGE	STRATIGRAPHIC UNIT
UPPER CRETACEOUS	Mesaverde Group
	Mancos Shale
LOWER CRETACEOUS	Dakota Sandstone
	Burro Canyon Formation
JURASSIC	Morrison Formation
	San Rafael Group
	Summerville (Wanakah) Fm
	Entrada Sandstone
	Carmel Formation
	Glen Canyon Group
	Navajo Sandstone
UPPER TRIASSIC	Kayenta Formation
	Wingate Sandstone
	Chinle Formation
	Shinarump Cgl Mbr
LOWER PERMIAN	Cutler Group
PENNSYLVANIAN	Hermosa Group
	Honaker Trail Formation
	Paradox Formation
	Ismay Member
	Desert Creek Member
	Akah Member
	Barker Creek Member
	Pinkerton Grain Formation
	Molas Formation
MISSISSIPPIAN	Leadville Limestone
DEVONIAN	Ouray Formation
	Elbert Formation
	Upper Ebert Member
	McCracken Sandstone Mbr
	Aneth Formation
UPPER CAMBRIAN	Ignacio Quartz
PRECAMBRIAN	Precambrian rocks

Figure 16. Stratigraphic section of the Paradox Basin. After Ambrose, 1998.

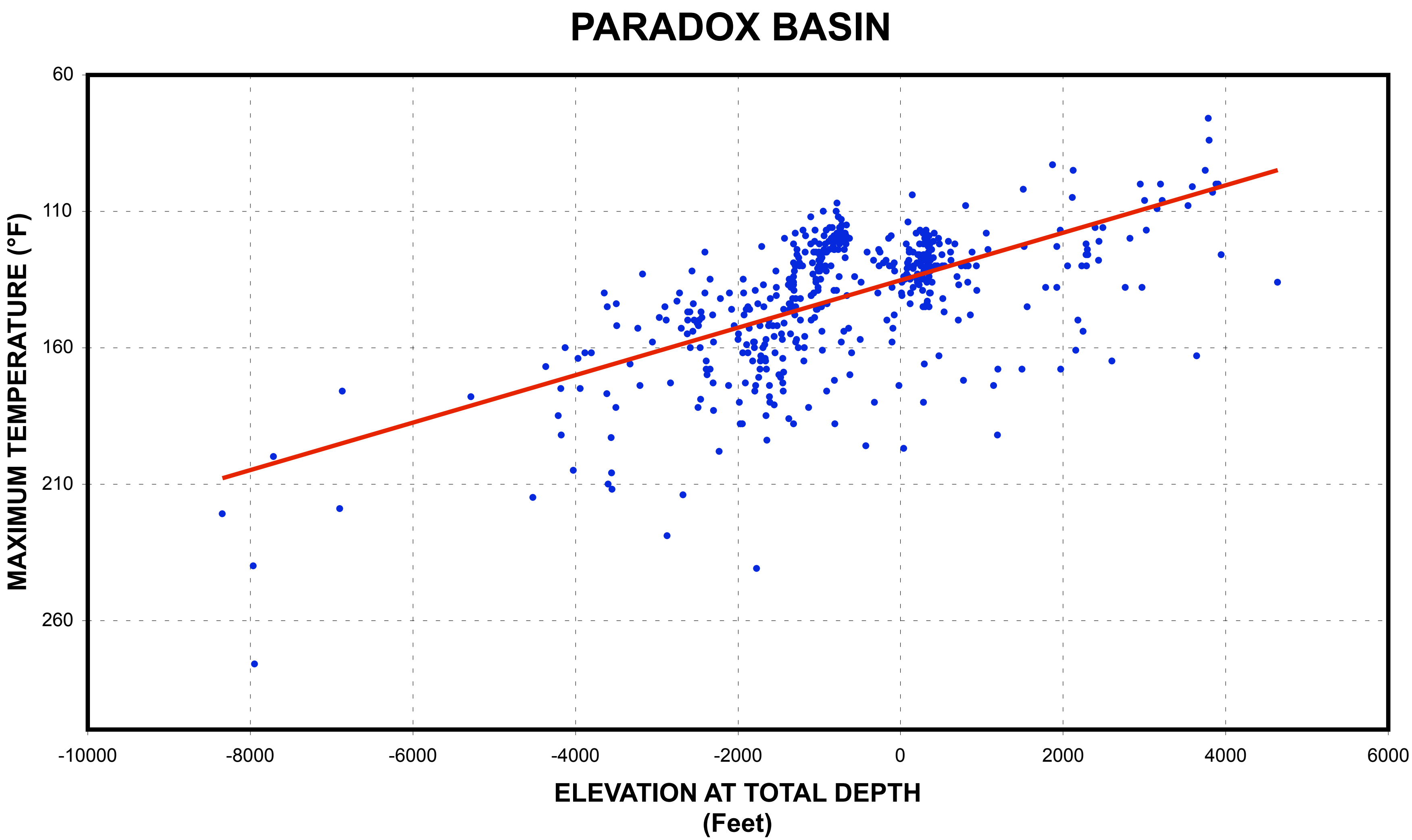

Figure 17. Plot of elevation at total depth-versus-maximum temperature, all wells.

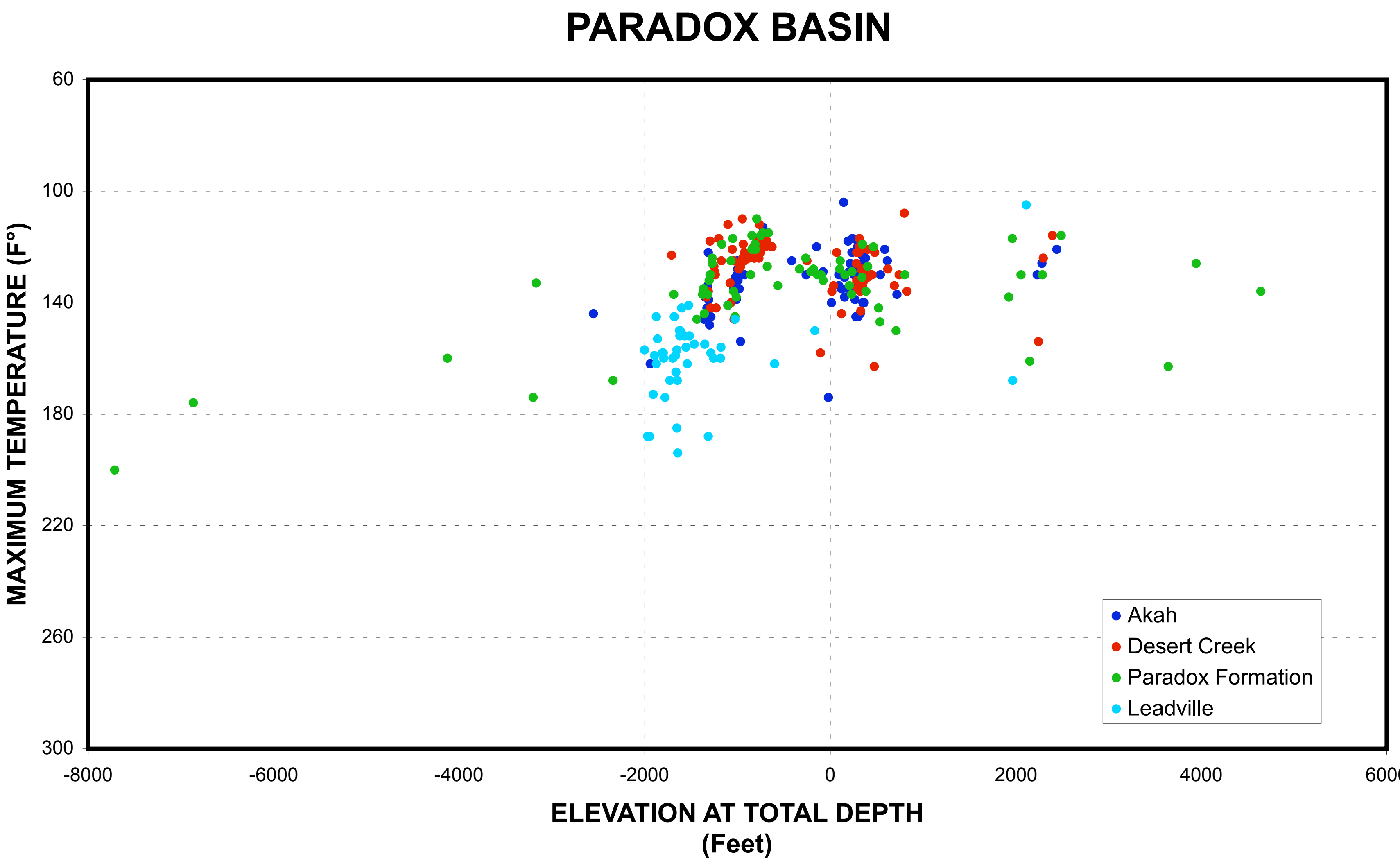

Figure 18. Plot of elevation at total depth-versus-maximum temperature, by formation.

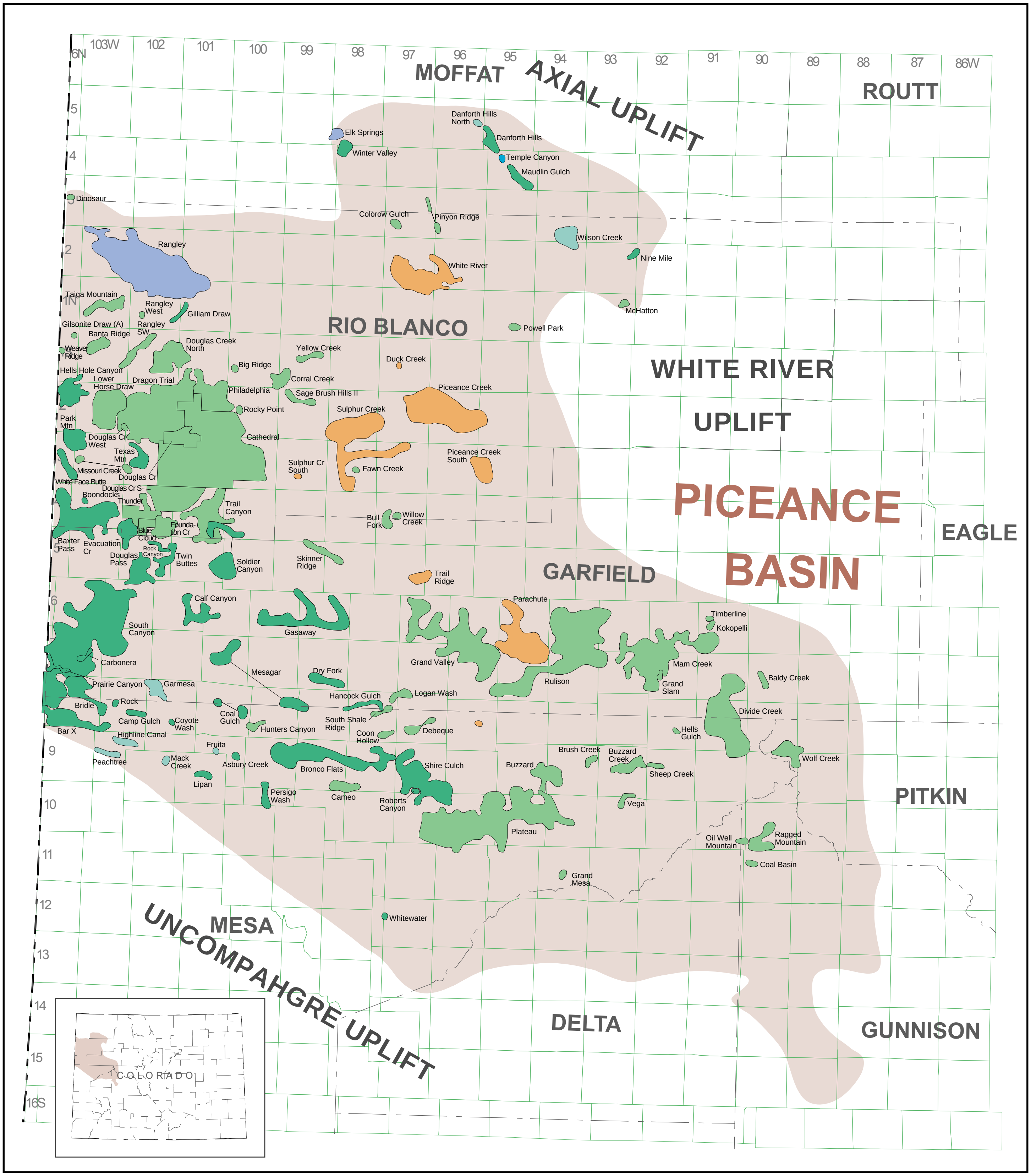

Figure 19. Map of the Piceance Basin. After Wray and others, 2002. Oil and gas fields indicated by outline.

PREDOMINANT AGE OF PRODUCTION of OIL and GAS FIELDS

- Tertiary
- Upper Cretaceous
- Lower Cretaceous
- Jurassic
- Jurassic-Triassic
- Triassic
- Permian
- Permian-Pennsylvanian
- Pennsylvanian
- Mississippian

PICEANCE BASIN

AGE	STRATIGRAPHIC UNIT
EOCENE	Unita Formation
	Green River Formation
	Parachute Creek Mbr
	Douglas Creek Mbr
	Wasatch Formation
PALEOCENE	Fort Union Formation
UPPER CRETACEOUS	Mesaverde Group
	Ohio Creek Mbr
	Williams Fork Formation
	Cameo zone
	Iles Formation
	Rollins Sandstone
	Coaaette Sandstone Mbr
	Corcoran Sandstone Mbr
	Sego Sandstone
	Castlegate Sandstone
	Mancos Shale
	Morapos (Mancos A) Ss
	Emery (Mancos B) Ss
	Meeker Sandstone
	Niobrara Formation
	Frontier Formation
LOWER CRETACEOUS	Mowry Shale (Benton Shale)
	Dakota Group
	Ceda Mountain Formation
UPPER JURASSIC	Morrison Formation
	Brushy Basin Mbr
	Salt Wash Mbr
MIDDLE JURASSIC	Curtis Formation
	Entrada (Sundance) Sandstone
LOWER JURASSIC	Navajo (Nugget) Sandstone
UPPER TRIASSIC	Chinle Formation
	Shinarump Ss Mbr
	Moenkopi Formation
UPPER PERMIAN	Phosphoria Formation
LOWER PERMIAN	Weber (Maroon) Sandstone
PENNSYLVANIAN	Minturn (Morgan) Formation
	Belden Shale
	Molas Formation
MISSISSIPPIAN	Leadville (Madison) Limestone
DEVONIAN	Chaffee Group
ORDOVICIAN	Manitou Formation
CAMBRIAN	Dotsero Formation
	Sawatch Sandstone
PRECAMBRIAN	Precambrian rocks

Figure 20. Stratigraphic section of the Piceance Basin. After Ambrose, 1998.

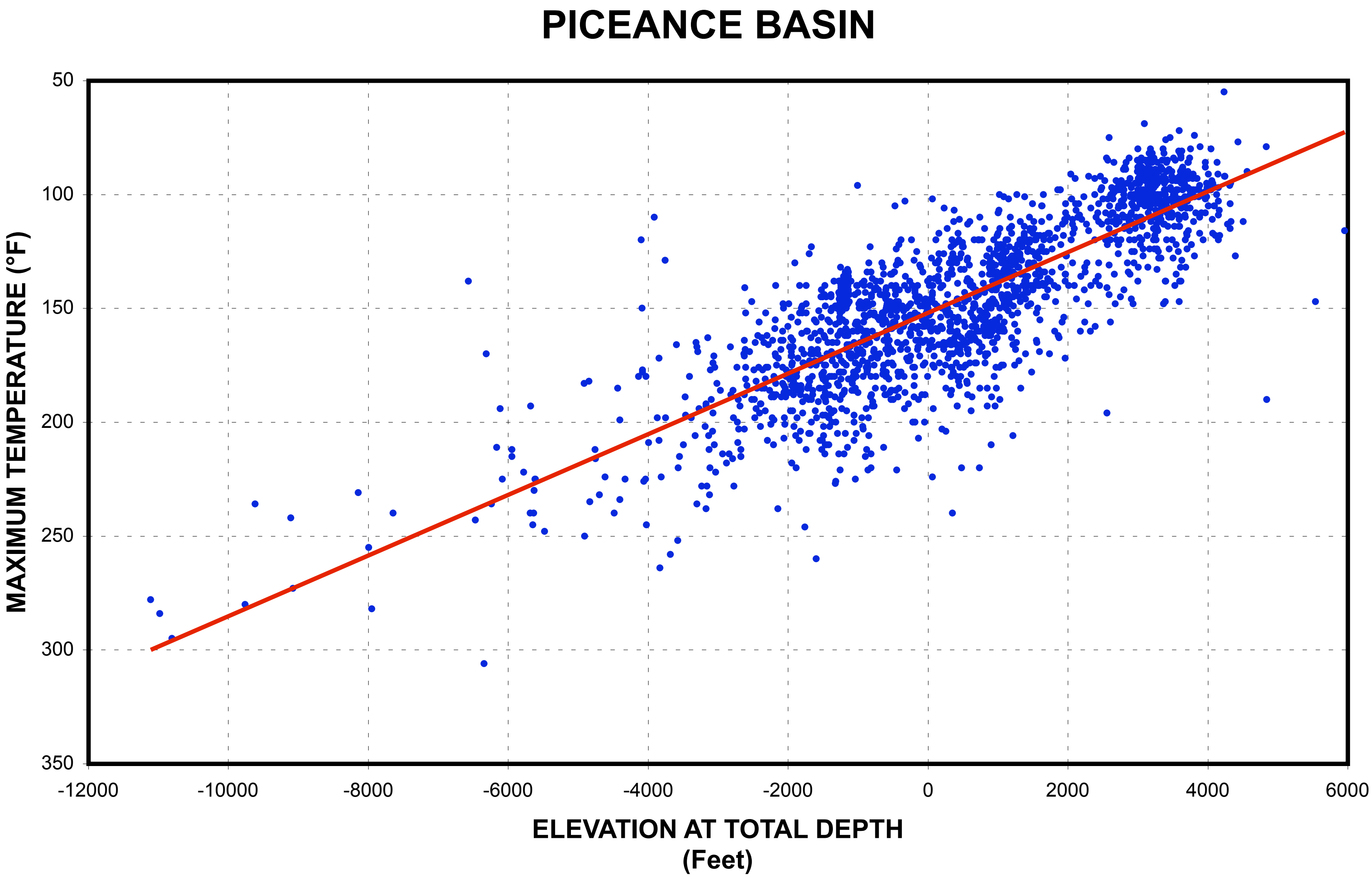

Figure 21. Plot of elevation at total depth-versus-maximum temperature, all wells.

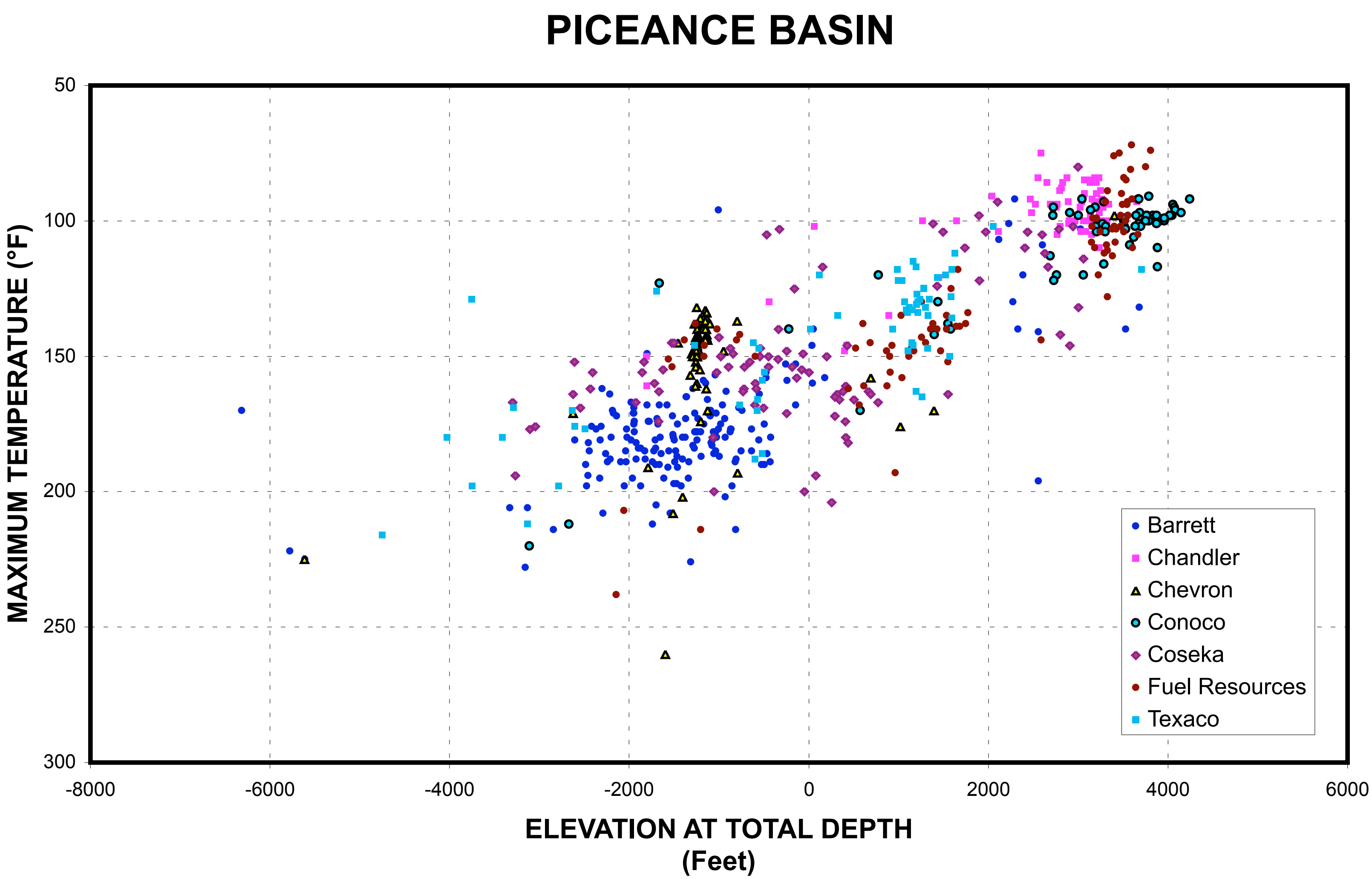

Figure 22. Plot of elevation at total depth-versus-maximum temperature, by operator.

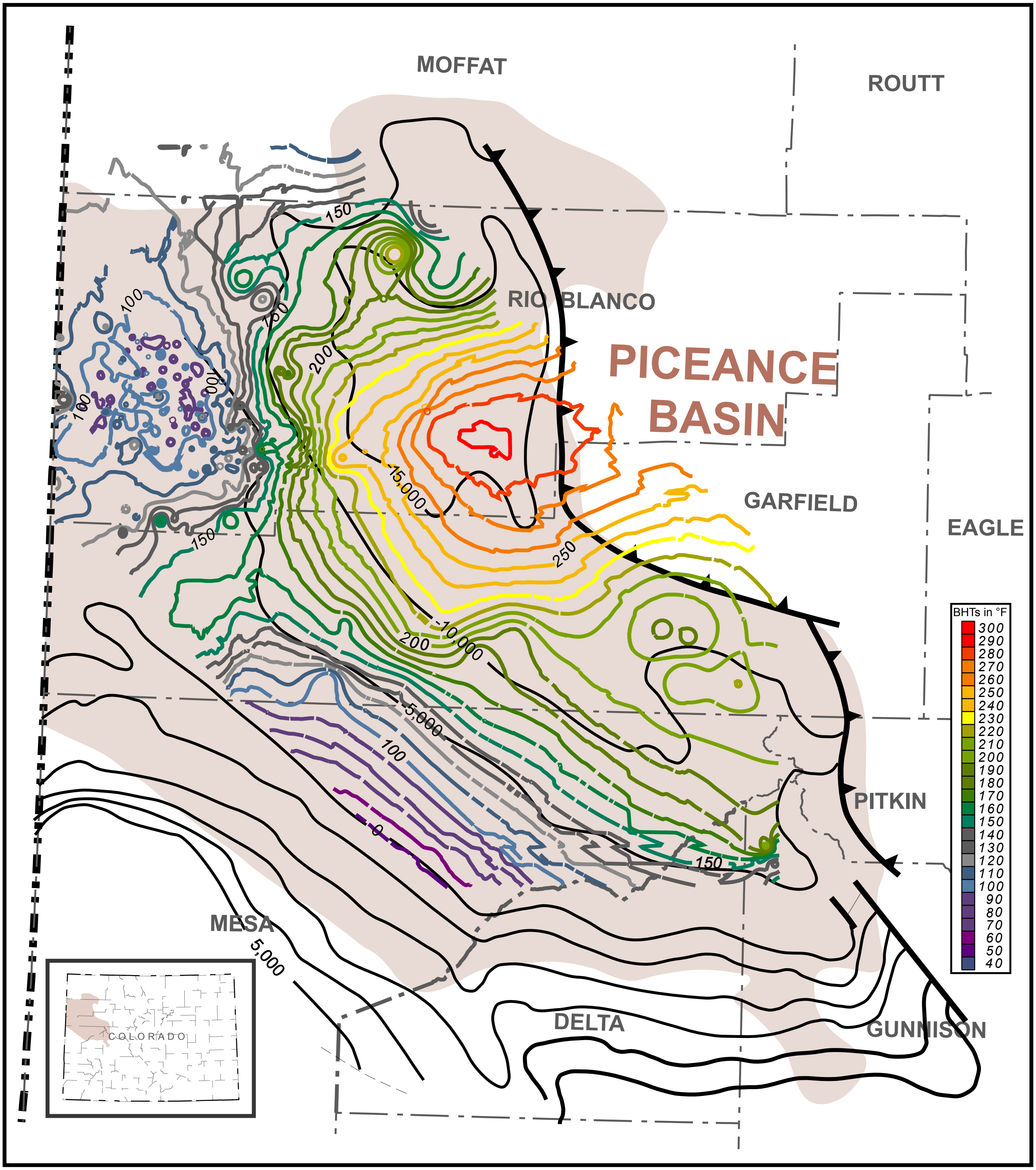

Figure 23. Contour of the BHTs of Piceance Basin wells, Mancos Shale at total depth, overlain by basement structure contours. After Hemborg, 1996. Structure contours in feet above and below sea level. Well data not shown because of high density.

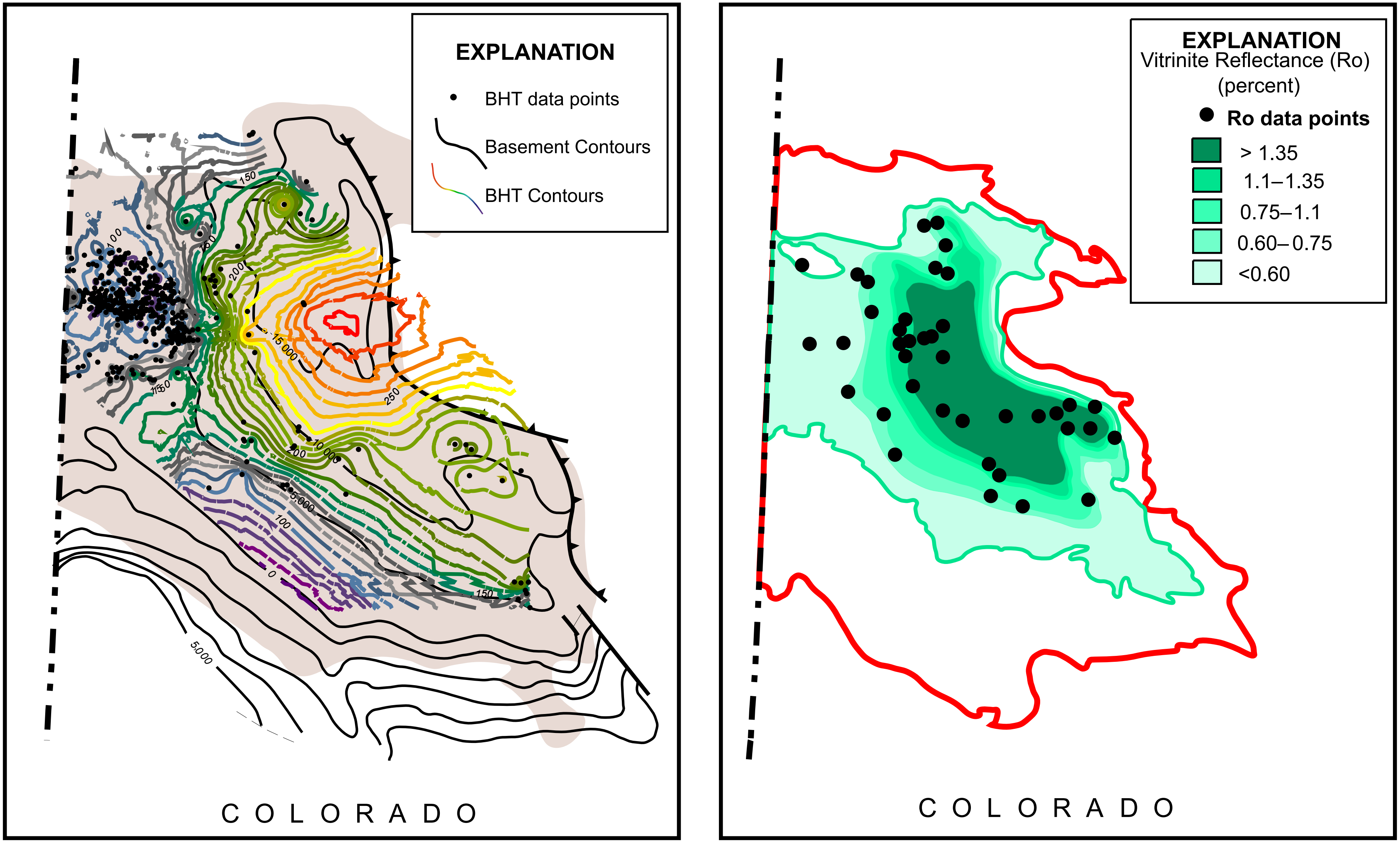

Figure 24. Comparison of the basement structure and BHT contours on the Mancos Shale with vitrinite isoreflectance (Ro) trends on the top of the Manco Shale, Piceance Basin (After Donatch and Carter, 2003).

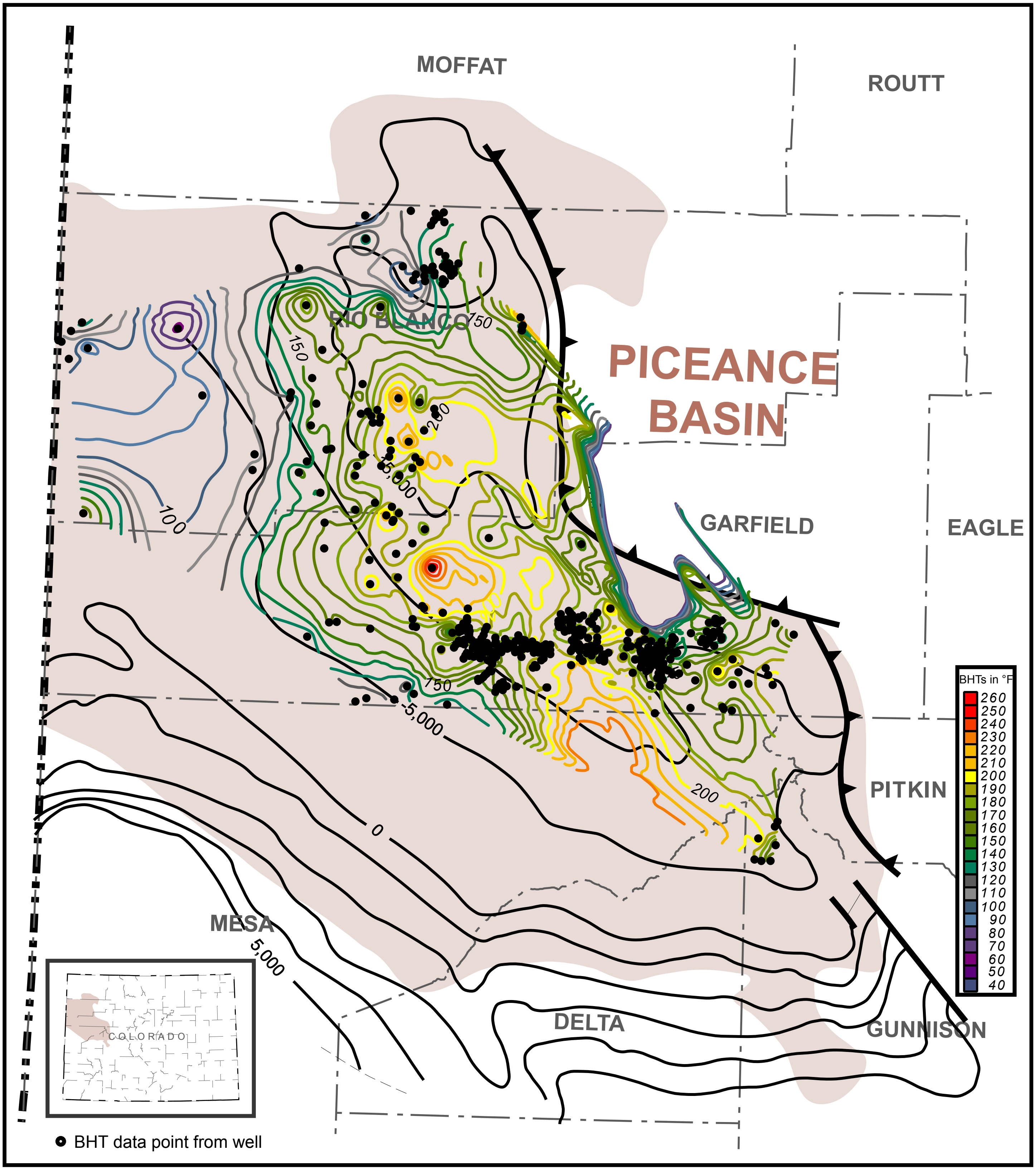

Figure 25. Contour map of the BHTs of Piceance Basin well, Mesaverde at total depth, overlain by basement structure contours. After Hemborg, 1996. Structure contours in feet above and below sea level.

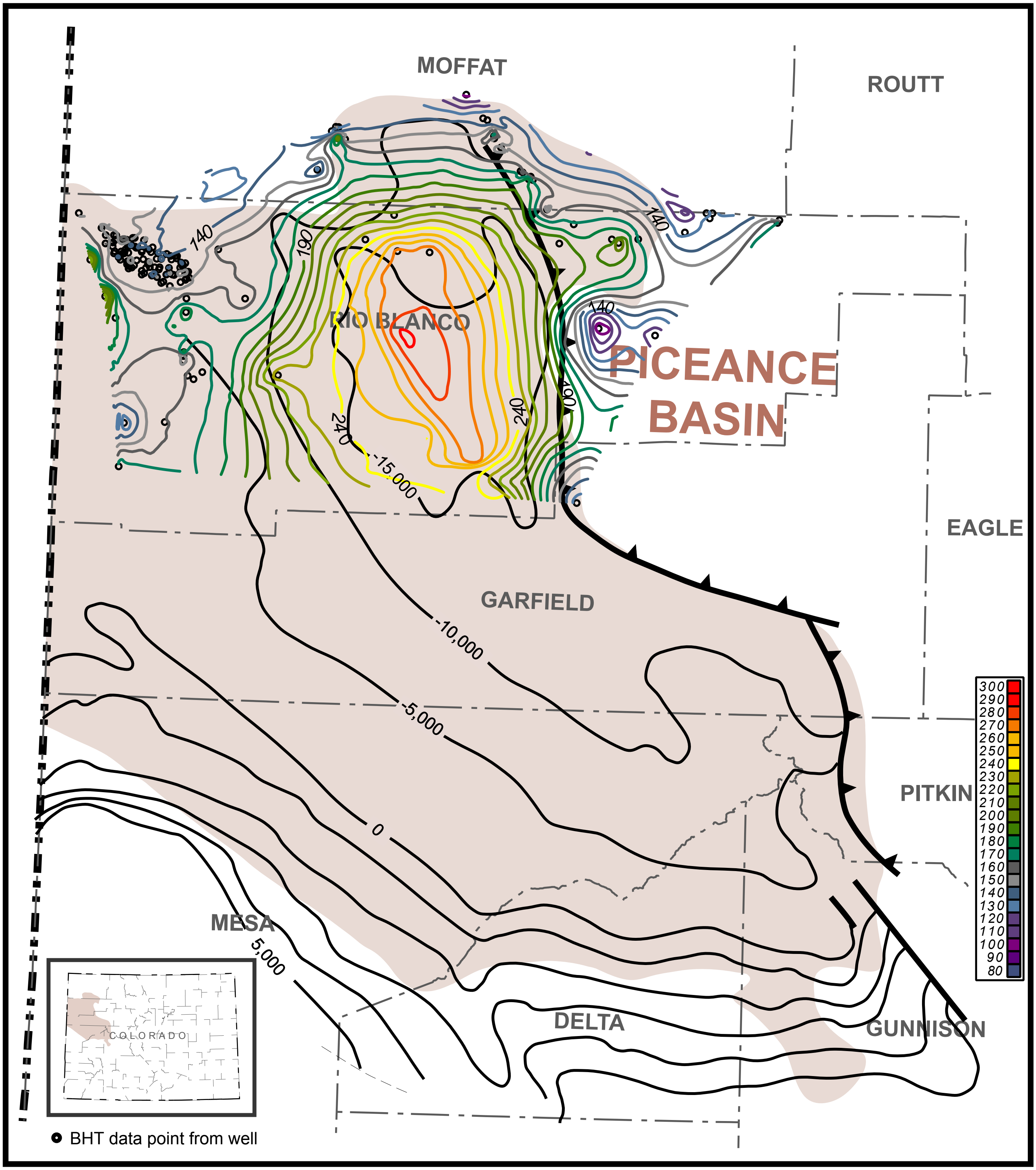

Figure 26. Contour map of the BHTs of Piceance Basin wells, Weber at total depth, overlain by basement structure contours. After Hemborg, 1996. Structure controus in feet above and below sea level.

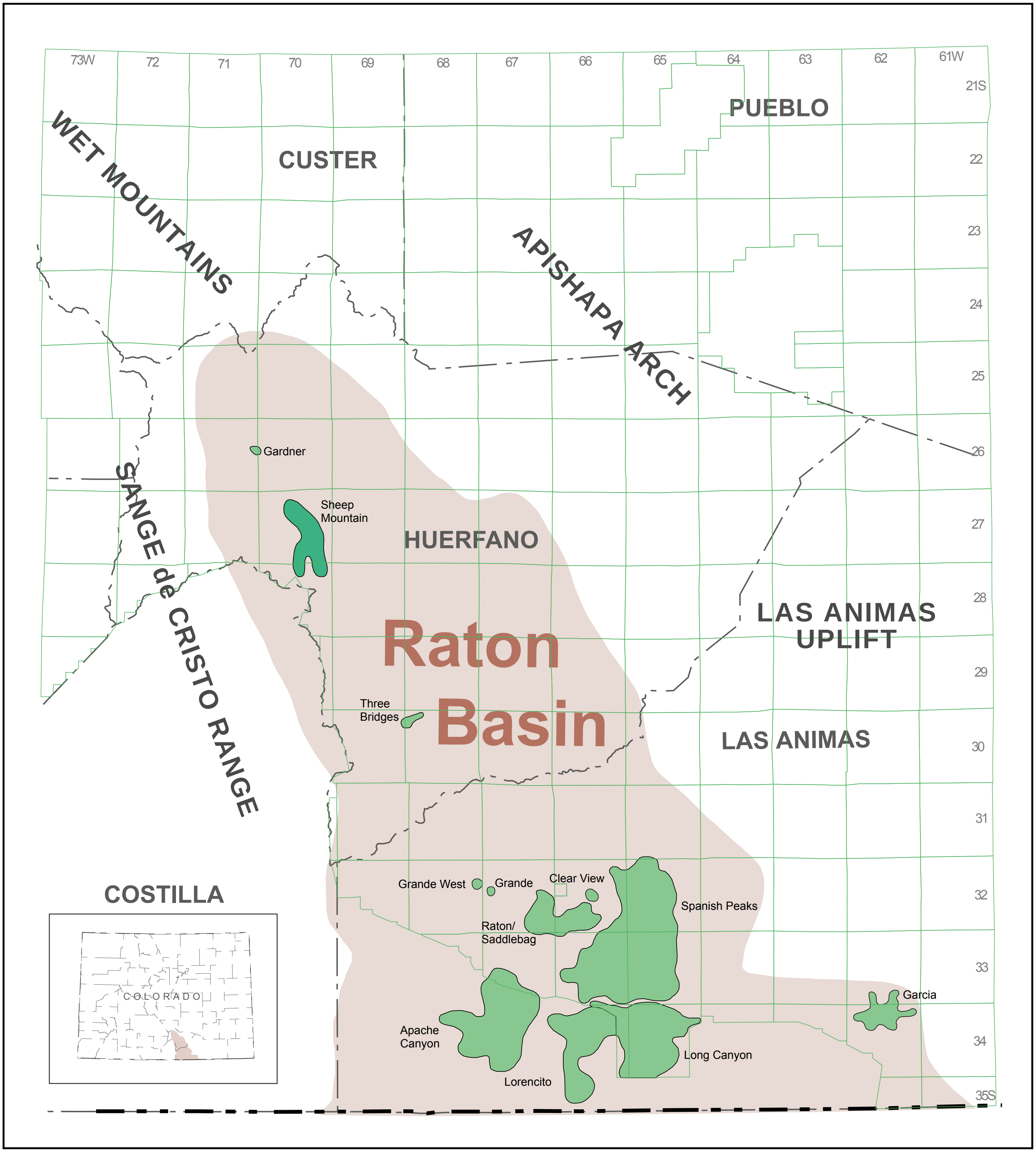

Figure 27. Map of the Raton Basin. After Wray and others, 2002. Oil and gas fields indicated by outline.

PREDOMINANT AGE OF PRODUCTION of OIL and GAS FIELDS

- Tertiary
- Upper Cretaceous
- Lower Cretaceous
- Jurassic
- Jurassic-Triassic
- Triassic
- Permian
- Permian-Pennsylvanian
- Pennsylvanian
- Mississippian

RATON BASIN

AGE	STRATIGRAPHIC UNIT
MIOCENE	Devils Hole Formation
OLIGOCENE	Farisita Formation
EOCENE	Huerfano Formation
	Cuchara Formation
PALEOCENE	Poison Canyon Formation
	Raton Formation
UPPER CRETACEOUS	Vermejo Formation
	Trinidad Sandstone
	Pierre Shale
	Niograra Formation
	Smoky Hill (Apishapa) Mbr
	Fort Hays (Timpas) Ls Mbr
	Benton Group
	Carlile Shale
	Codell Sandstone Mbr
	Greenhorn Limestone
	Graneros Shale
LOWER CRETACEOUS	Dakota Sandstone
	Purgatorre (Lakota) Formation
JURASSIC	Morrison Formation
	Ralston Creek (Wanakah) Fm
	Entrada Sandstone
TRIASSIC	Dockum Group
	Chinle Formation
	Santa Fosa Formation
PERMIAN	Glorietta Fm (Lyons)
	Yeso Fm (Sumner Group)
	Sangre De Cristo (Fountain) Fm
PENNSYLVANIAN	Madera Formation
PRECAMBRIAN	Precambrian rocks

Figure 28. Stratigraphic section of the Raton Basin. After Ambrose, 1998.

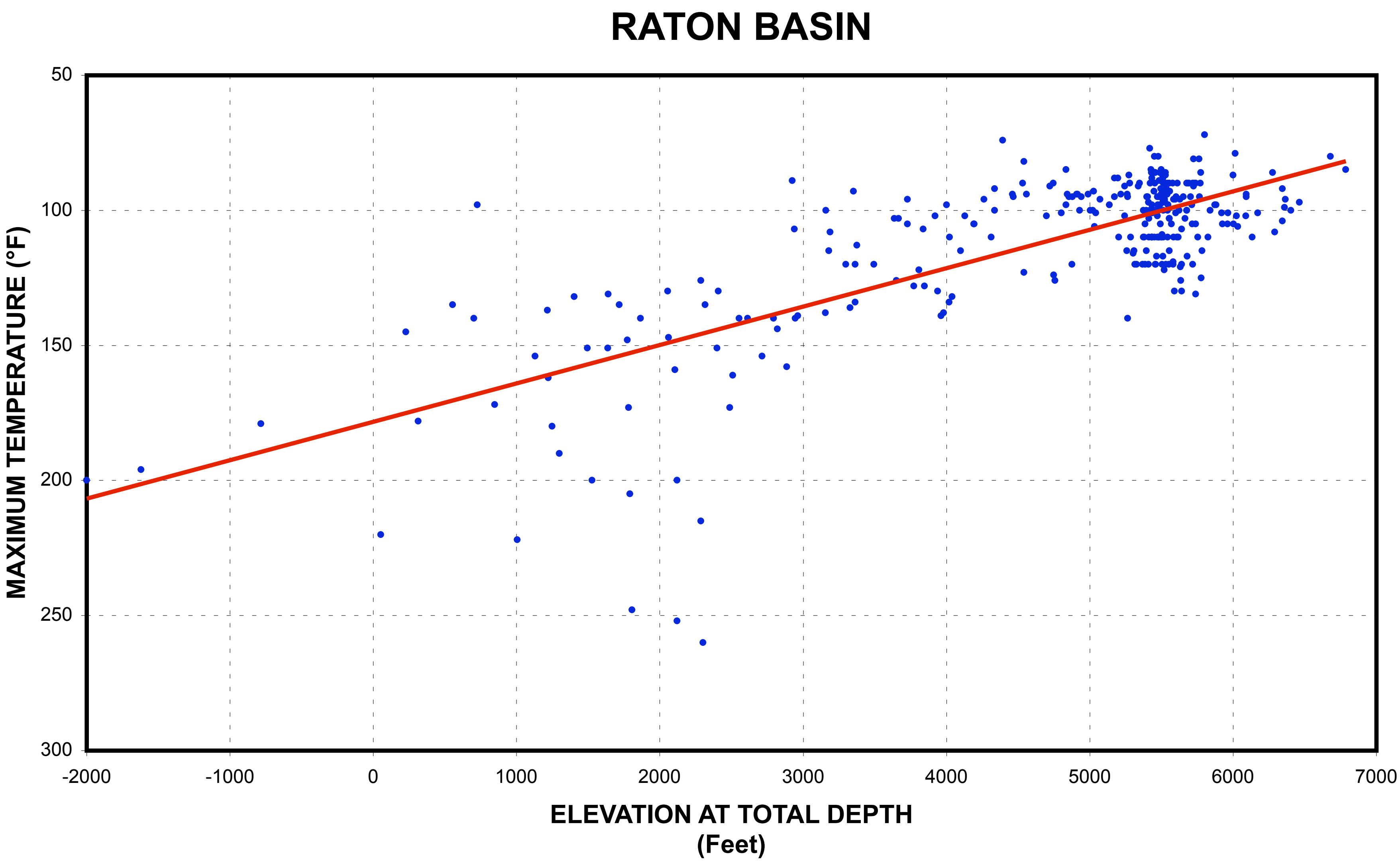

Figure 29. Plot of elevation at total depth-versus-maximum temperature, all wells.

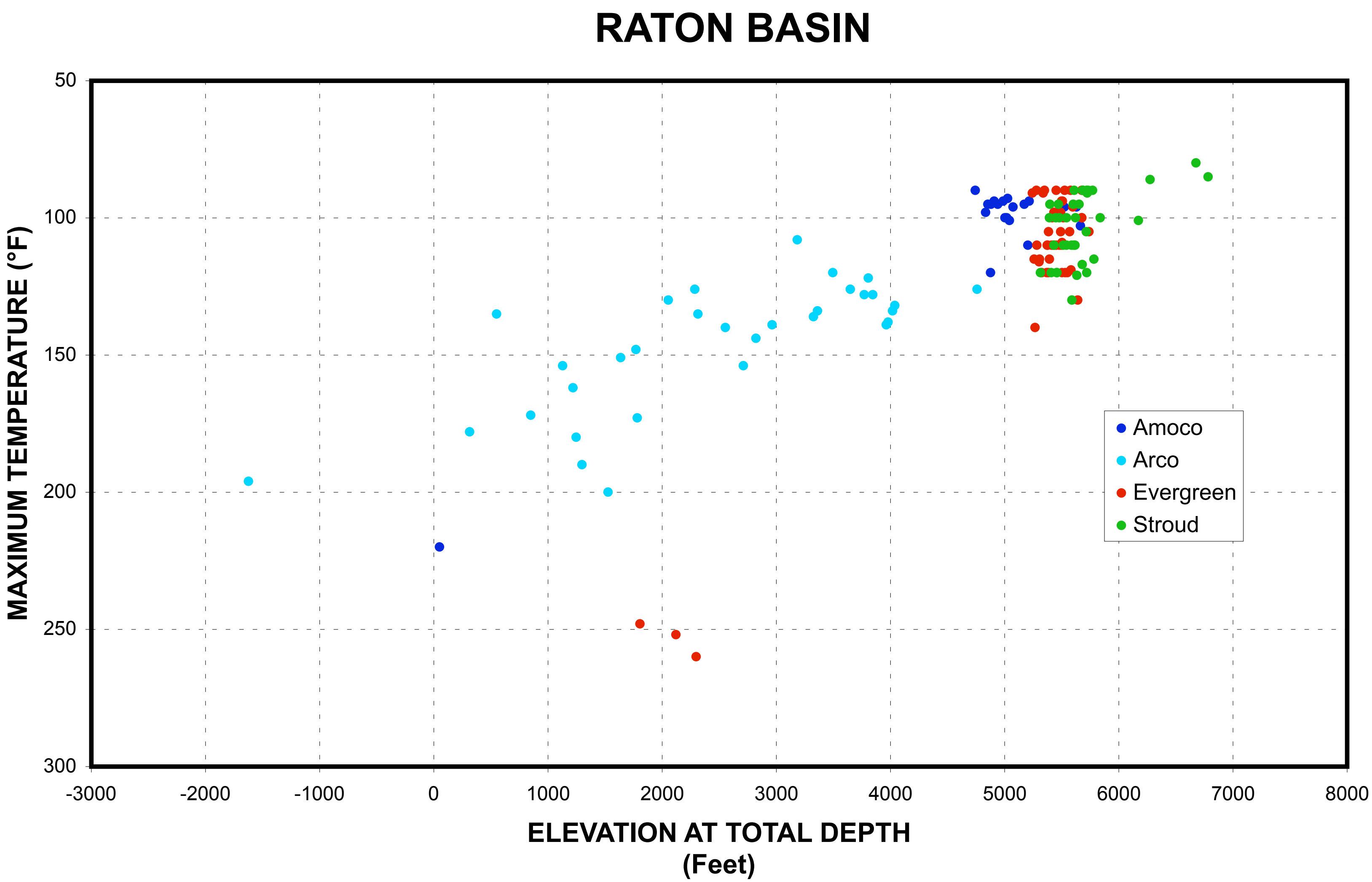

Figure 30. Plot of elevation at total depth-versus-maximum temperature, by operator.

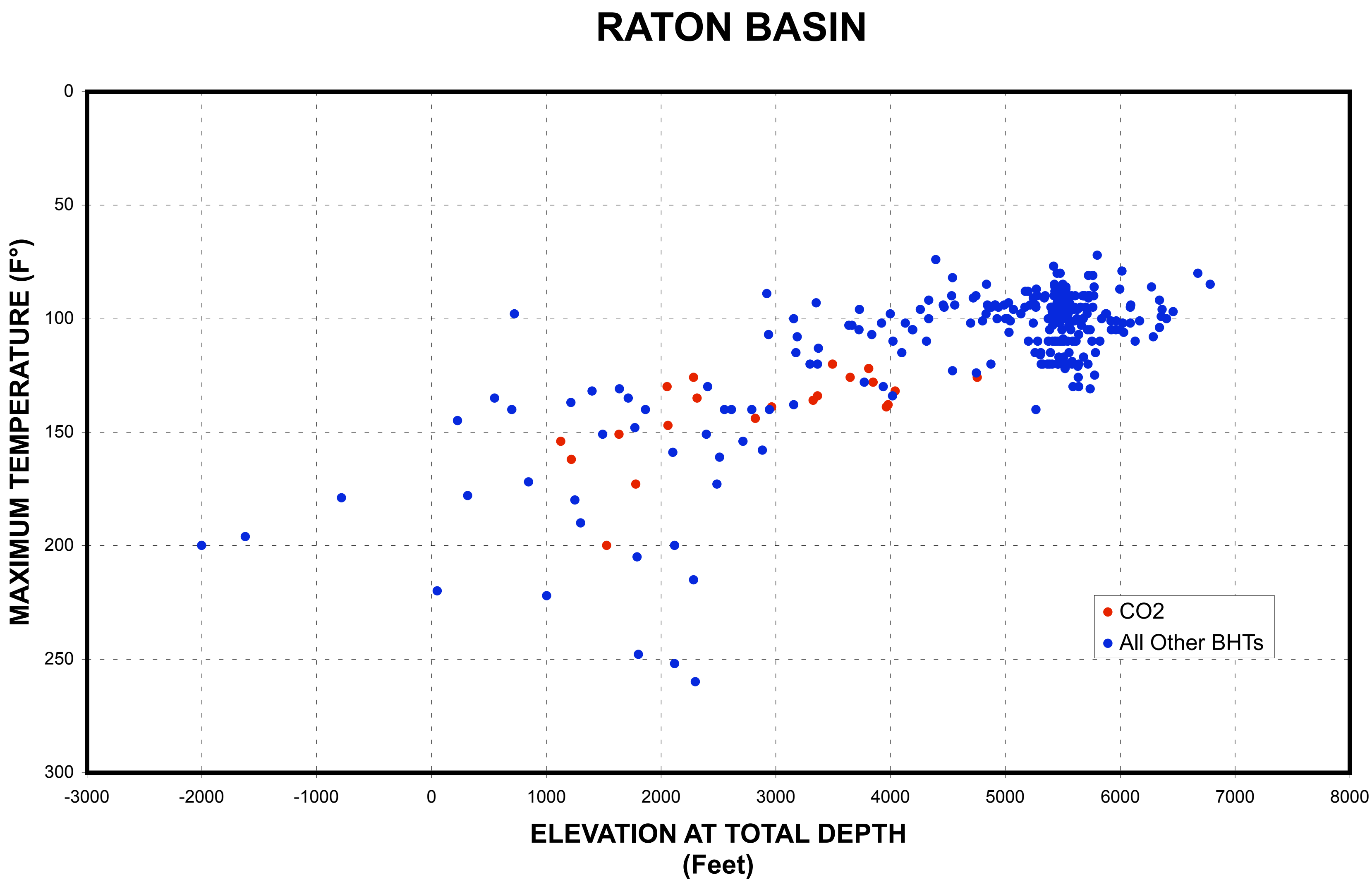

Figure 31. Plot of elevation-versus-maximum temperature, comparing CO_2 wells with all other wells.

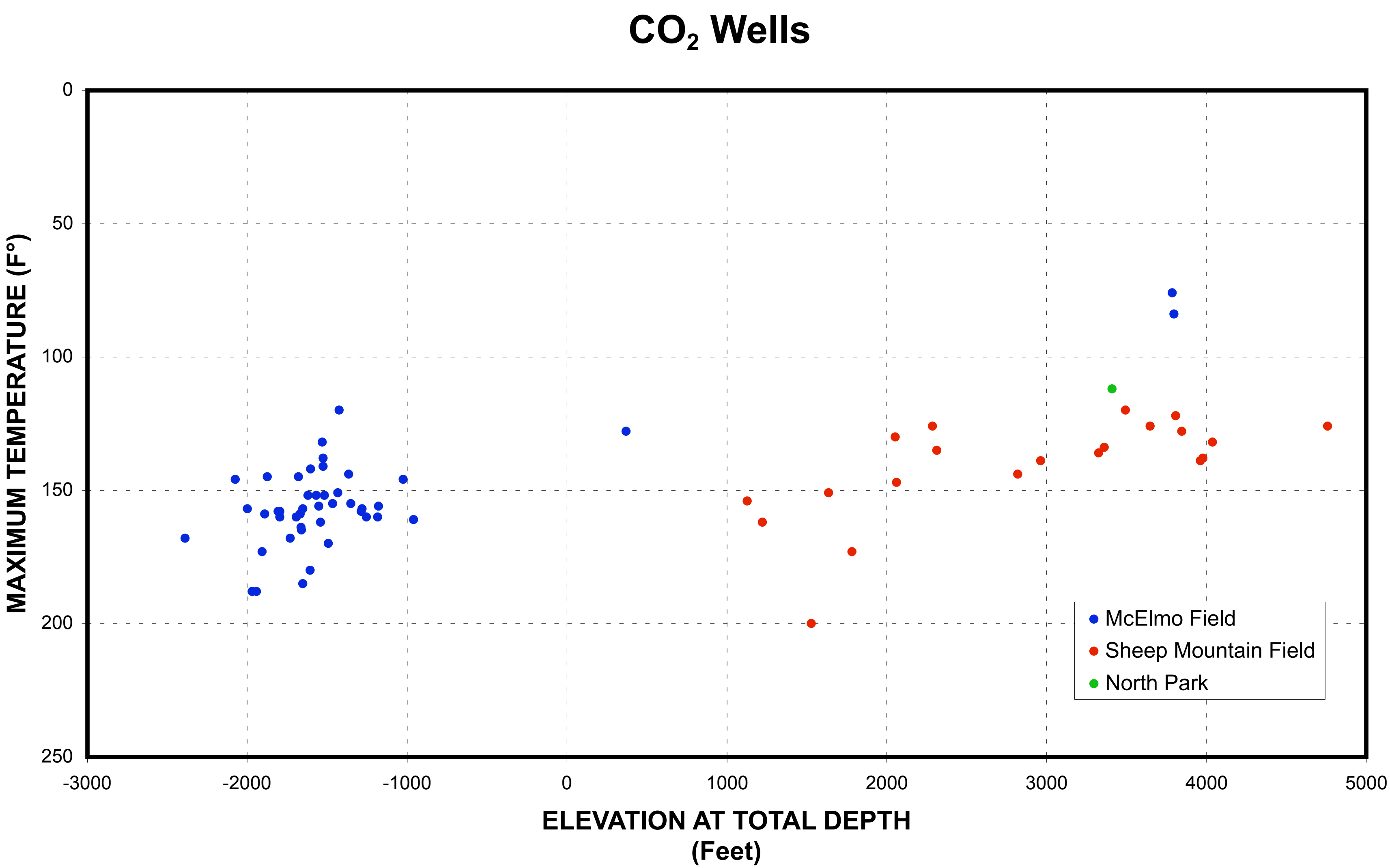

Figure 32. Elevation at total depth-versus-maximum temperature, CO_2 wells.

Figure 33. Map of the Sand Wash Basin. After Wray and others, 2002. Oil and gas fields indicated by outline.

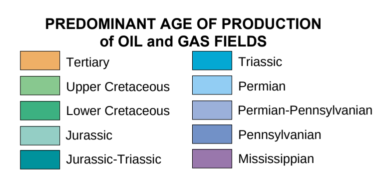

SAND WASH BASIN

AGE	STRATIGRAPHIC UNIT
MIOCENE	Browns Park Formation
EOCENE	Green River Formation
	Wasatch Formation
PALEOCENE	Fort Union Formation
UPPER CRETACEOUS	Lance Formation
	Fox Hills Formation
	Lewis Shale
	Mesaverde Group
	Williams Fork Fm
	(Almond Ericson)
	Iles (Rock Springs) Fm
	Mancos Shale
	Morapos Ss Mbr
	Niobrara Mbr
	Carlile (Benton) Mbr
	Frontier Sandstone
LOWER CRETACEOUS	Mowry Shale
	Dakota Group
JURASSIC	Morrison Formation
	Curtis Formation
	Entrada Sandstone
	Carmel Sandstone
	Nugget Sandstone
TRIASSIC	Chinle Formation
	Shinarump Ss Mbr
	Moenkopi Formation
UPPER PERMIAN	Phosphoria (Park City) Fm
LOWER PERMIAN	Weber Sandstone
PENNSYLVANIAN	Morgan (Belden) Formation
MISSISSIPPIAN	Madison or Leadville Ls
DEVONIAN	Chaffee Group
	Dyer Formation
	Parting Sandstone
UPPER CAMBRIAN	Lodore Formation
PRECAMBRIAN	Precambrian rocks

Figure 34. Stratigraphic section of the Sand Wash Basin. After Ambrose, 1998.

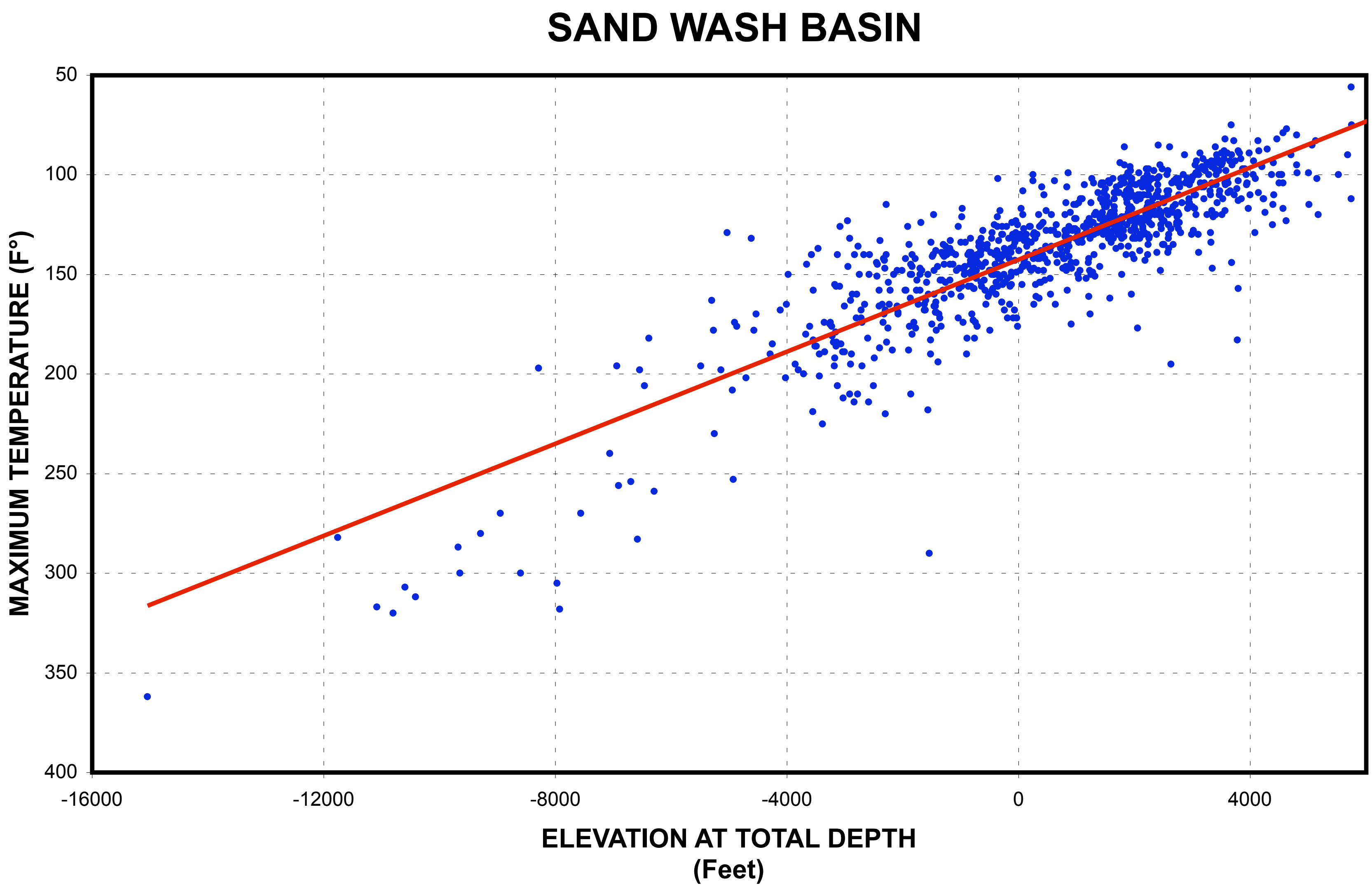

Figure 35. Plot of elevation at total depth-versus-maximum temperature, all wells.

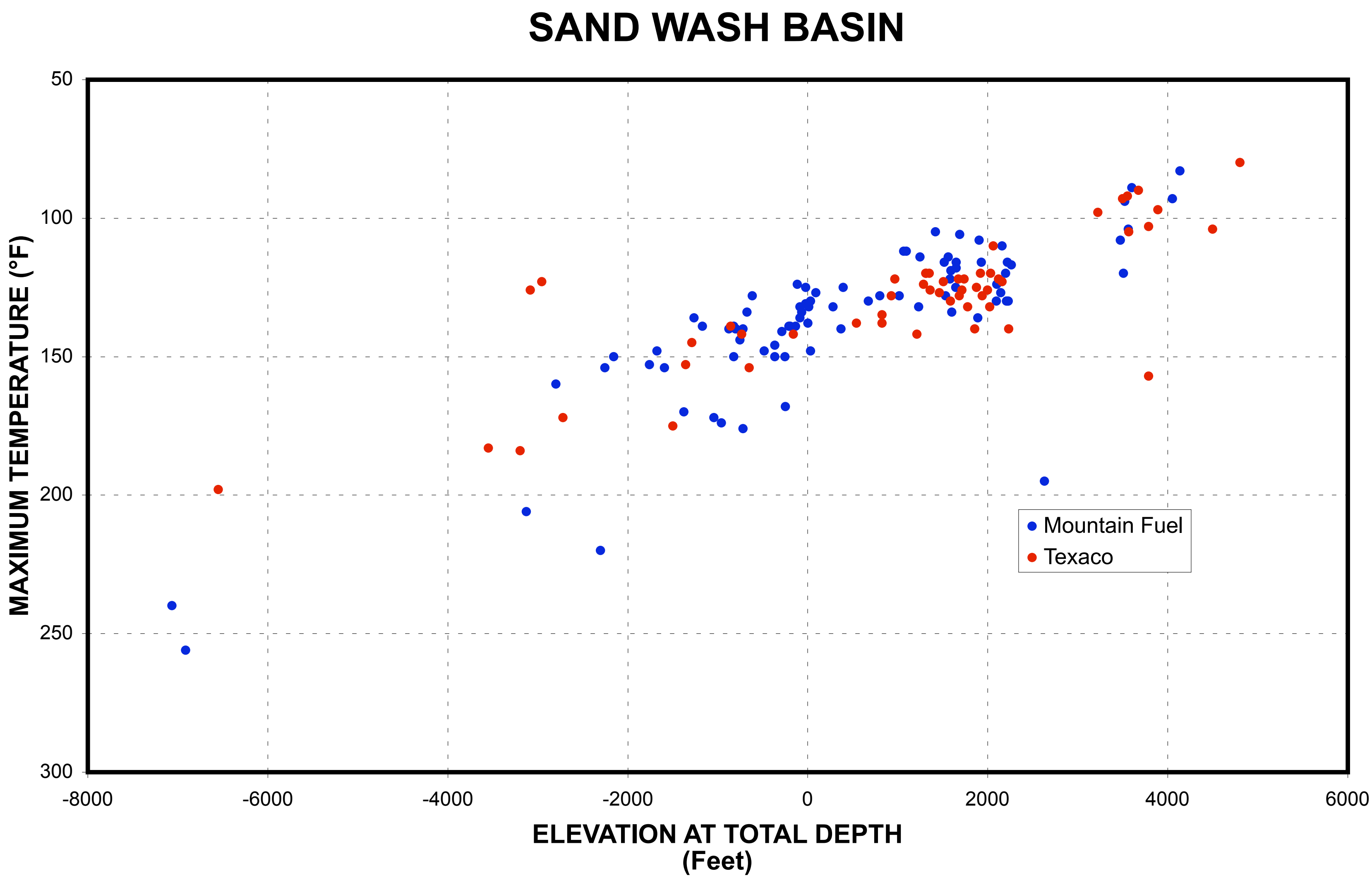

Figure 36. Plot of elevation at total depth-versus-maximum temperature, by operator.

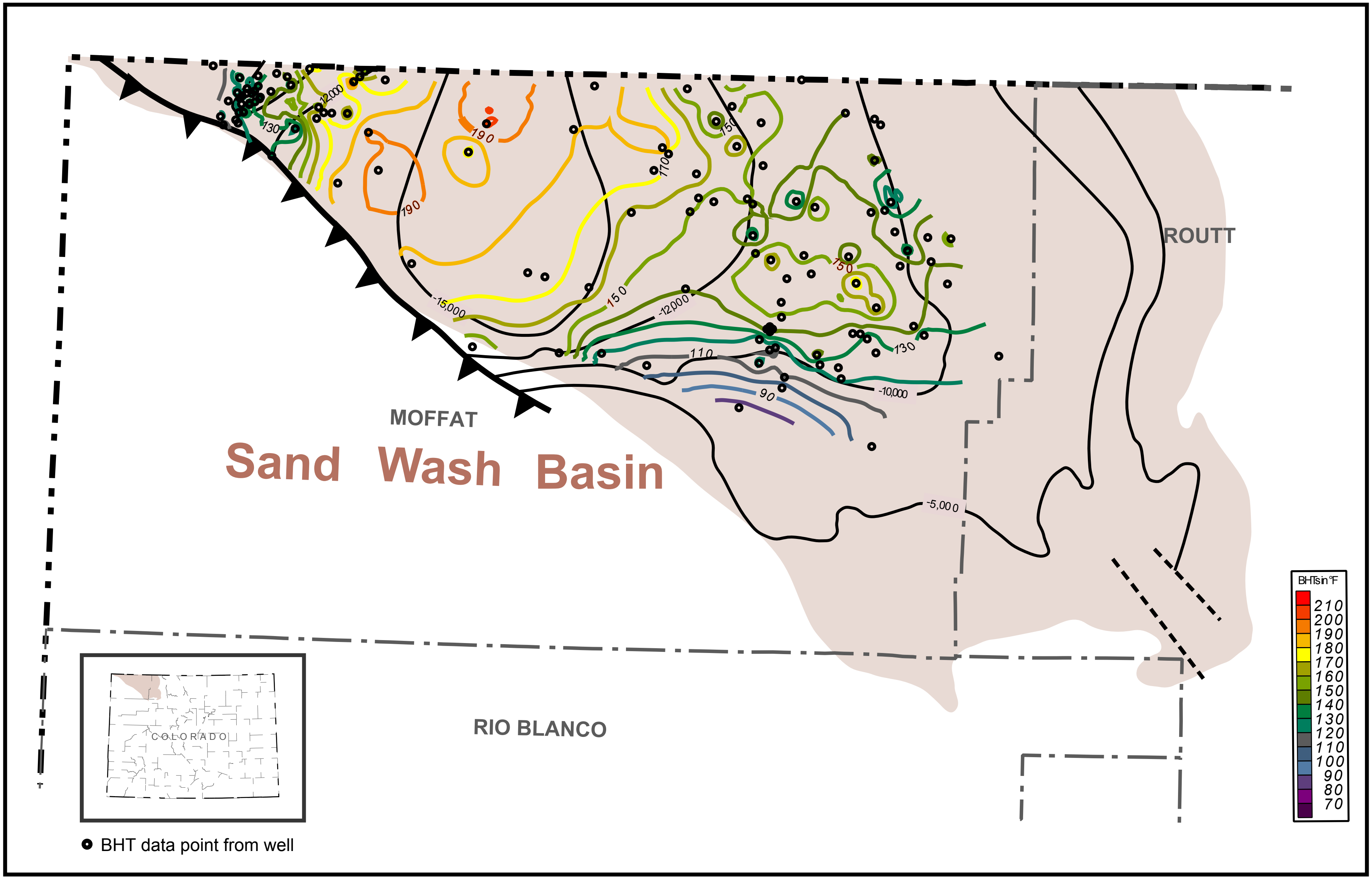

Figure 37. Contour map of BHTs of the Sand Wash Basin wells, Mesaverde at total depth, overlain by basement structure contours. After Hembor, 1996. Structure contours are in feet below sea level.